LETTER

doi:10.1038/nature11292

Inland thinning of West Antarctic Ice Sheet steered along subglacial rifts

Robert G. Bingham[1], Fausto Ferraccioli[2], Edward C. King[2], Robert D. Larter[2], Hamish D. Pritchard[2], Andrew M. Smith[2] & David G. Vaughan[2]

Current ice loss from the West Antarctic Ice Sheet (WAIS) accounts for about ten per cent of observed global sea-level rise[1]. Losses are dominated by dynamic thinning, in which forcings by oceanic or atmospheric perturbations to the ice margin lead to an accelerated thinning of ice along the coastline[2–5]. Although central to improving projections of future ice-sheet contributions to global sea-level rise, the incorporation of dynamic thinning into models has been restricted by lack of knowledge of basal topography and subglacial geology so that the rate and ultimate extent of potential WAIS retreat remains difficult to quantify. Here we report the discovery of a subglacial basin under Ferrigno Ice Stream up to 1.5 kilometres deep that connects the ice-sheet interior to the Bellingshausen Sea margin, and whose existence profoundly affects ice loss. We use a suite of ice-penetrating radar, magnetic and gravity measurements to propose a rift origin for the basin in association with the wider development of the West Antarctic rift system. The Ferrigno rift, overdeepened by glacial erosion, is a conduit which fed a major palaeo-ice stream on the adjacent continental shelf during glacial maxima[6]. The palaeo-ice stream, in turn, eroded the 'Belgica' trough, which today routes warm open-ocean water back to the ice front[7] to reinforce dynamic thinning. We show that dynamic thinning from both the Bellingshausen and Amundsen Sea region is being steered back to the ice-sheet interior along rift basins. We conclude that rift basins that cut across the WAIS margin can rapidly transmit coastally perturbed change inland, thereby promoting ice-sheet instability.

Many independent satellite sensors have been used to gauge the recent mass imbalance of the Antarctic ice sheet, thereby to assess the rate of its contribution to global sea-level rise[2–4,8]. These studies highlight coastal regions of the WAIS as major contributors to current sea-level rise through a process termed "dynamic thinning"[2]. Such a region is Pine Island Glacier in the Amundsen Sea embayment, where gradual ungrounding and thinning of the floating ice shelf, potentially triggered by oceanic forcing, have induced progressive drawdown and thinning of inland ice[3–5]. These observations have reignited concerns that the wider WAIS is progressing towards a predicted collapse within the next few centuries, increasing the need to understand the fundamental influences on its dynamic behaviour.

Theory suggests that the stability of WAIS is controlled by the subglacial topographic configuration, with landward-deepening basins favouring runaway retreat inland[9]. The subglacial geology and crustal structure of the West Antarctic rift system (WARS; Fig. 1a) may also influence ice dynamics[10–12]. Sedimentary basins underlie the onset of some ice streams in the Ross Sea embayment[13,14] and their initiation may be affected by elevated geothermal heat flux linked to inferred recent volcanism[10,15]. Yet, for the Bellingshausen Sea embayment, currently one of the most rapidly thinning parts of the WAIS (Fig. 1b), the subglacial topography and geological setting that may influence ice-sheet behaviour have remained largely unknown. Here we analyse new geophysical data sets from inland of the Bellingshausen Sea and demonstrate that propagation of ice thinning towards the interior is promoted where narrow rift basins associated with a northeasterly extension of the WARS connect to the ocean.

Our data set comprises the first systematic radar survey of Ferrigno Ice Stream (FIS; 85° W, 74° S), a 14,000-km^2 ice-drainage catchment clearly identified by satellite altimetry as the most pronounced 'hotspot' of dynamic thinning along the Bellingshausen Sea margin of the WAIS (Fig. 1b). Data were collected by over-snow survey between November 2009 and February 2010, and supplemented by airborne data collected by the US NASA Operation IceBridge programme in 2009. The only previous measurements of ice thickness across the entire 150 km × 115 km catchment were a sparse set of reconnaissance seismic and gravity spot-depths obtained 50 years previously along exploratory traverses, and a handful of airborne radar measurements collected on the way to other locations (Fig. 1c). Our new view of the bed beneath FIS reveals a narrow subglacial basin with a maximum depth of about 1,500 m below sea level striking northeast–southwest through the catchment. Viewed in the wider context (Fig. 1d), using the most recent compilations of subglacial topography and offshore bathymetry, together with new analyses of magnetic and gravity data, we can see that the basin forms part of a major fault system that connects rift basins in the interior of the WARS to Eltanin Bay[16,17] (Supplementary Fig. 1a–c).

Radar-derived bed echoes across FIS (Fig. 2a, Supplementary Figs 2–4) deviate in form from the U-shaped parabolic profile that represents the 'pure' product of glacial erosion[18]. Instead, the steeply dipping, approximately 1-km-high basin flanks and the flat basin floor resemble classical rift structures[19]. Further supporting evidence for a rift origin is the dip of the bed away from the basin flanks (Fig. 2a, Supplementary Figs 3 and 4), consistent with the tilting of fault blocks and footwall uplift.

Aeromagnetic anomaly data[20] (Fig. 3, Supplementary Figs 5–7) reveal that the Ferrigno rift formed close to the boundary between a highly magnetic magmatic arc province that lies primarily offshore in the FIS region (and that extends from the Antarctic Peninsula to Thurston Island) and a more weakly magnetic province onshore. The latter is interpreted as a back-arc region, where the early WARS developed about 105–90 million years (Myr) ago[21]. This part of the WARS was then reactivated during inferred dextral transtensional motion between 48 Myr ago and 26 Myr ago[17]. Depth to magnetic sources help to constrain our gravity and magnetic models and indicate that the narrow Ferrigno rift contains about 1 km of sedimentary infill (Fig. 3c, d, Supplementary Figs 8 and 9). Three-dimensional inversion of satellite gravity data indicates that the crust is around 25–21 km thick beneath the Ferrigno rift and the adjacent Siple Trough region (Fig. 1d and Supplementary Figs 1c and 10). This is similar to the 22–24-km-thick crust in the western Amundsen Sea embayment[22] and the approximately 20-km-thick crust beneath the Pine Island rift[23] and the Bentley Subglacial Trench[10]. These new findings lead us to conclude that the Ferrigno rift region was affected by crustal thinning associated with the WARS. There is, however, no magnetic evidence in support of widespread Cenozoic magmatism

[1]School of Geosciences, University of Aberdeen, Elphinstone Road, Aberdeen, AB24 3UF, UK. [2]British Antarctic Survey, High Cross, Madingley Road, Cambridge, CB3 0ET, UK.

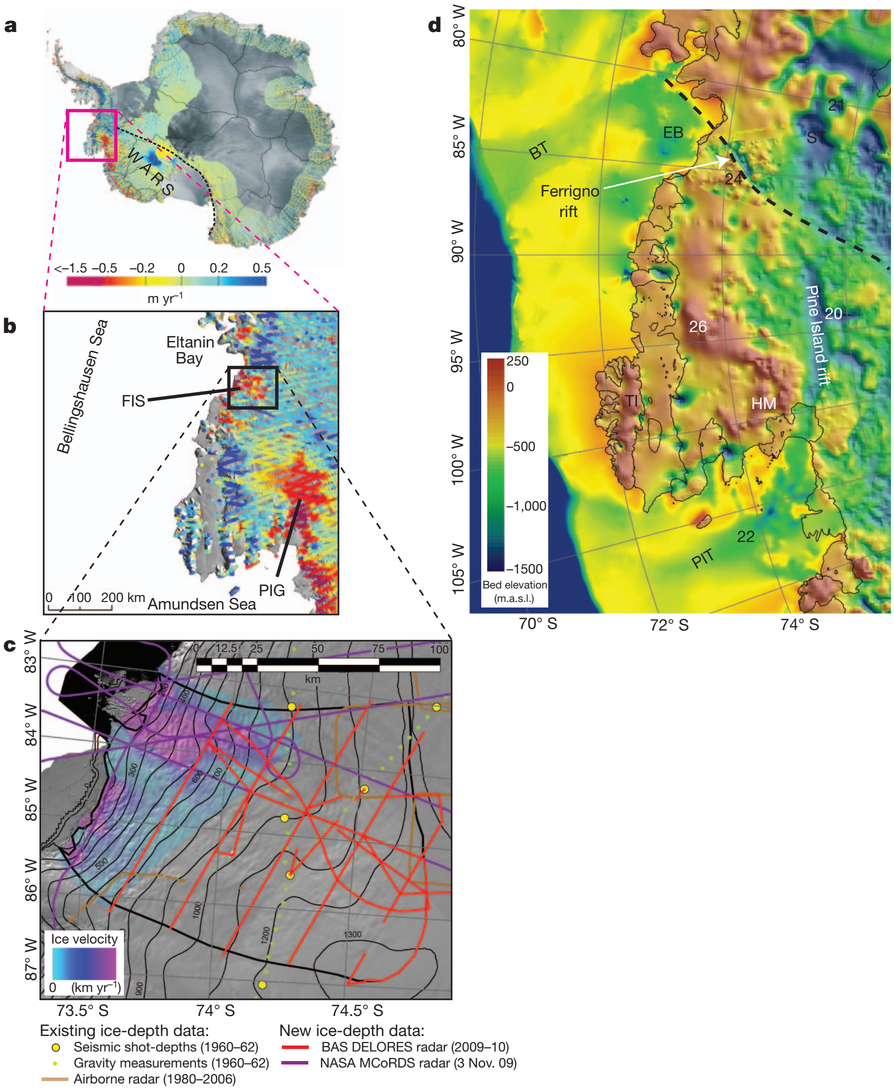

Figure 1 | Surface change, survey coverage, and subglacial topography for the Bellingshausen Sea sector of West Antarctica. **a**, Rate of surface elevation change along ICESat tracks measured between 2003 and 2007; superimposed over the Landsat Image Mosaic of Antarctica (grey shading). Regions coloured red in the Bellingshausen and Amundsen Sea sectors of West Antarctica exhibit strong ice surface lowering attributable to dynamic thinning. The flank of the WARS is annotated with a black dashed curve. **b**, Enlargement of the boxed area in **a**, with major geographical features labelled. **c**, Enlargement of the boxed area in **b**, showing orientation of new radar tracks obtained across FIS in 2009–10; pre-existing ice-depth measurement locations are also marked. The black line demarcates the Ferrigno catchment. Also shown are satellite-derived ice velocities for the lower portion only of the catchment (ref. 28), 100-m surface contours and background imagery from the Landsat Image Mosaic of Antarctica. **d**, Regional subglacial topography mosaicked from our new data set for FIS (see Fig. 3a and Supplementary Fig. 3 for detail) and refs 29 and 30. The black dashed line highlights a major fault system that we propose connects rift basins in the interior of the WARS to Eltanin Bay (EB). BT, Belgica trough; PIT, Pine Island trough; ST, Siple trough; TI, Thurston Island; HM, Hudson Mountains. Numbers are estimates of crustal thickness (in kilometres) in the WARS derived from inversion of Bouguer gravity anomaly data and seismic data[11,22]. m.a.s.l., metres above sea level.

close to the Ferrigno rift, in contrast to the Ross and Amundsen Sea sectors of the WARS (Supplementary Figs 1b and 11).

A recently suggested middle-Miocene (about 17–13 My ago) change in plate motion between East and West Antarctica[24] has significant implications for how we interpret the Ferrigno rift in relation to inferred Neogene (23–2.5 Myr ago) rifting processes (Fig. 1d and Supplementary Fig. 1). A Neogene rifting stage and glacial overdeepening may account for the deepest basins within the WARS, including the Byrd Subglacial Basin and the Bentley Subglacial Trench[17]. The low effective elastic thickness in the Pine Island rift[23] is similar to values observed over recent rifts[19], supporting the hypothesis of a Neogene rifting phase there. All these features that are inferred to be Neogene rifts may be kinematically linked (Fig. 1d and Supplementary Fig. 10).

We note that the Ferrigno rift broadly aligns with the inland extent and distribution of the dynamic-thinning signal observed at the ice surface with altimetry (Fig. 3a). Modern ice flow also follows the direction of the rift (Fig. 1c). These associations suggest that dynamic thinning of ice towards the West Antarctic interior may be promoted where ice is underlain by glacially overdeepened rift basins associated with development of the WARS.

We propose two factors that can explain the observed correlation of inland dynamic thinning with subglacial rifting. First, the sedimentary infill we identified within the Ferrigno rift (Fig. 3c, d) probably facilitated formation of a deforming bed (see ref. 14 for an example) that would promote enhanced ice flow and thinning. Second, elevated geothermal heat flux has been measured within the Terror rift (Supplementary Fig. 1a), a narrow rift basin that was active in Neogene times[25]. If the Ferrigno rift were similarly active in the Neogene, as we hypothesize, then enhanced geothermal heat flux linked to focused crustal thinning would probably occur beneath FIS. This would lead to excess generation of subglacial meltwater, which in turn would lubricate the bedrock, accelerate ice flow and thereby exacerbate dynamic thinning effects. Although incidences of rifts exploited and overdeepened by ice-stream flow have been noted elsewhere[13,26,27], in none of these cases has an influence on contemporary ice thinning been noted. What seems to be required to promote dynamic thinning inland is a coincidence of a deep rift basin cutting across the ice-sheet margin and inflow of warm ocean water onto the continental shelf.

We conclude that the WAIS is most at threat from the inward incursion of dynamic thinning along glacially overdeepened rifts that extend both into the Amundsen and Bellingshausen seas. The Ferrigno rift connects through to Eltanin Bay, where the lack of an ice shelf today and in the observational record implicates the sustained presence of relatively warm air and/or ocean water[7], providing a forcing mechanism for the dynamic thinning of coastal ice. Without favourable subglacial conditions further inland, this dynamic thinning would be limited to the coastal fringes as on other parts of the Antarctic margin; instead, the deep inland reach of the Ferrigno rift facilitates a strong coupling between the oceanic front and the deeper ice-sheet interior (Fig. 3a and Supplementary Fig. 12). The situation at the FIS evokes that of Pine Island Glacier, where, over two decades of observation, the access of warm ocean water has instigated dynamic thinning at the

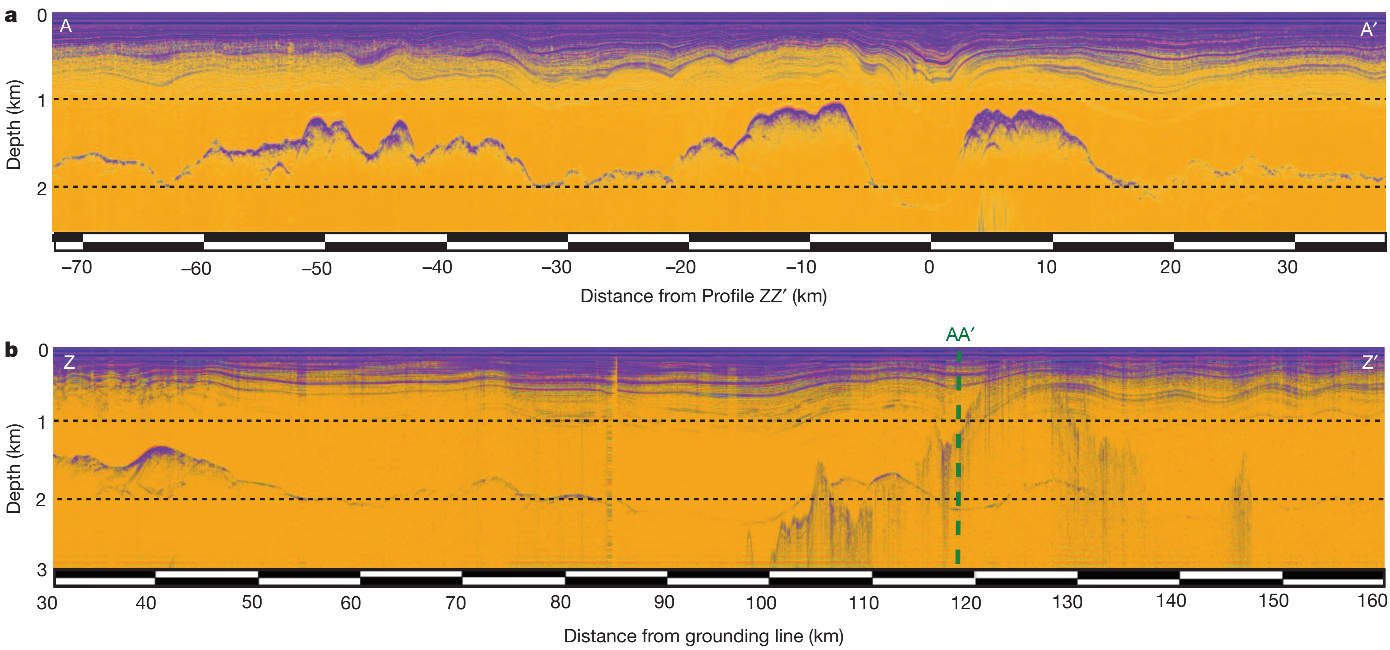

Figure 2 | Radar profiles showing morphology of Ferrigno Ice Stream bed. **a**, 110-km-long radar profile across the Ferrigno catchment transverse to the main axis of ice flow (profile AA′ marked on Fig. 3a). Distance scale is marked relative to the ice-stream (rift) centreline (path followed by profile ZZ′ in **b**). Ice flow is towards the reader. The vertical scales in **a** and **b** show depth below present ice surface. **b**, 130-km-long radar profile collected along the main trench ZZ′ (location marked on Fig. 3a). Distance scale is marked in kilometres from the grounding line; the crossing point of profile AA′ is shown. Sporadic interference patterns between 100 km and 147 km result from 'sideswipe' returns from valley walls as the radar passed over a narrowing in the trench.

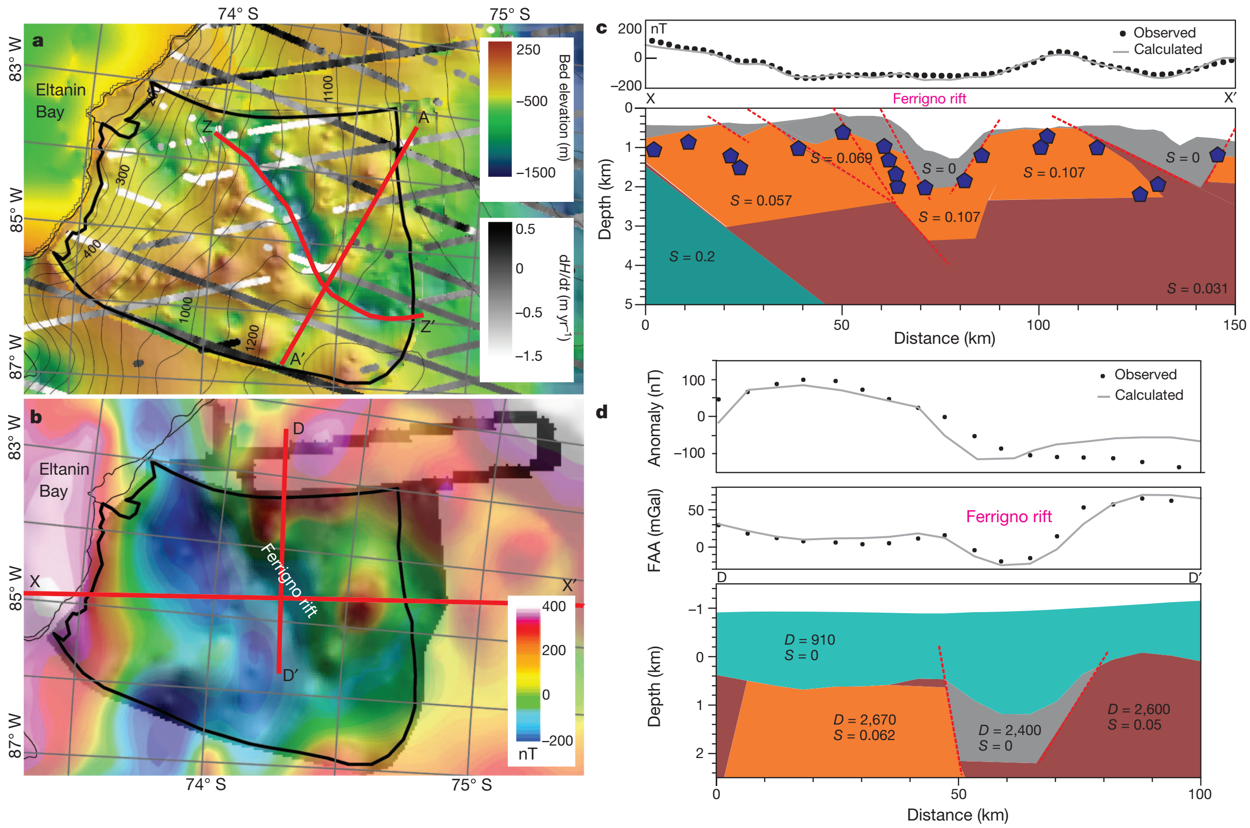

Figure 3 | Dynamic thinning of the ice sheet steered along a subglacial rift. **a**, Rate of surface ice elevation change measured between 2003 and 2007 along ICESat tracks (greyscale) superimposed over subglacial topography, showing enhanced thinning in the interior over the Ferrigno rift region. Black contours with labels show surface topography. Red lines show radar profiles in Fig. 2. **b**, The same area, reduced to the pole aeromagnetic anomaly map (colour scale, partially transparent), with new Ferrigno subglacial topography underneath. Note the northeast–southwest-oriented magnetic low that aligns with the Ferrigno rift. Red lines show the location of our magnetic and gravity models of the Ferrigno rift. **c**, Magnetic model of the Ferrigno rift. Blue symbols show the results of depth to magnetic source calculations that help constrain the model; the numbers denote magnetic susceptibilities. **d**, Combined gravity and magnetic model, indicating an approximately 1-km-thick sedimentary infill in the Ferrigno rift. Magnetic susceptibilities and densities are labelled as S (dimensionless) and D (kg m^{-3}) respectively.

grounding line, followed by propagation of ice drawdown deep along the Pine Island rift[3,23]. A radar profile we collected directly along the main axis of FIS (Fig. 2b) shows the bed deepening inland for about 70 km from the lower reaches. This leaves much of the upper catchment of FIS vulnerable to impending drawdown and retreat analogous to that of Pine Island Glacier, and demonstrates that the risk to the WAIS from dynamic thinning extends beyond the Amundsen Sea embayment.

Overall, the recent changes being witnessed today in West Antarctica represent not simply a short-term ice-sheet response to climate warming, but form part of a wider, sustained and complex system of interactions between tectonic activity, glacial landscape modification, and oceanic and atmospheric change. Over millennia, ice streams such as FIS and Pine Island Glacier have exploited rift structures and, over several glacial maxima, focused flow into palaeo-ice streams that have eroded troughs over the continental shelf such as the Belgica and Pine Island troughs (Fig. 1d). The Pine Island trough itself exploits a tectonic lineament caused by former rifting[22]; the Belgica trough also aligns with a northwest–southeast trending scarp on the inner continental shelf that runs at right angles to FIS and is probably imposed on a major tectonic lineament (Fig. 1d). These 'rift-directed' offshore troughs now form the putative routes through which warm open-ocean waters penetrate back over the continental shelf to attack the ice margin. Overdeepened rift basins onshore are now steering the transmission of this dynamic-thinning perturbation even further back towards the interior of West Antarctica, with likely consequences for ice-sheet stability.

METHODS SUMMARY

Our radar survey of FIS represents the only over-snow exploration over the region since two traverses immediately following the International Geophysical Year 50 years previously. It also comprises the first systematic survey (to our knowledge) of any of the WAIS catchments fringing the Bellingshausen Sea. Radar data were collected with the British Antarctic Survey DELORES system, a 2-MHz monopulse 'DEep-LOoking Radio Echo Sounder' with a pulse-repetition rate of 1 kHz and a digitization period of 10 ns. Tying this into dual-frequency global positioning system (GPS) for navigational fixing, we measured ice thickness at 7.5-m intervals along tracks, obtaining a total of 250,970 ice-thickness points. Assuming radar wave speed through ice of 168.5 m μs^{-1}, these were converted to bed elevations with estimated $\pm$3-m vertical resolution (see the file named ferrigno_delores.txt in the Supplementary Information). We also incorporated 17,793 further ice-thickness measurements obtained over parts of FIS on 3 November 2009 by the US NASA Operation IceBridge programme 140–230 MHz Multichannel Coherent Radar Depth Sounder (MCoRDS) (publicly available on http://nsidc.org/icebridge/portal/). We used these measurements, and the small amount of existing earlier ice-thickness measurements (http://www.antarctica.ac.uk//bas_research/data/access/bedmap/), to interpolate bed elevations over a 1-km grid mesh. We provide the final grid file used for this paper, ferrigno_topogrid_1km.txt in the Supplementary Information.

A reconnaissance aeromagnetic survey was made across the region in 1986–1987 (ref. 20), after which no further data were acquired. We reprocessed these data (see the file named mag_Drape3500_redp.XYZ in the Supplementary Information) and analysed them together with land gravity data to derive new models of the Ferrigno rift and estimate the thickness of its sedimentary infill. To assess crustal thickness beneath the WARS we applied three-dimensional inversion to satellite gravity data and airborne gravity data over the adjacent catchment of Pine Island Glacier.

Received 29 March; accepted 7 June 2012.

1. Meier, M. F. *et al.* Glaciers dominate eustatic sea-level rise in the 21st century. *Science* **317,** 1064–1067 (2007).
2. Pritchard, H. D., Arthern, R. J., Vaughan, D. G. & Edwards, L. A. Extensive dynamic thinning on the margins of the Greenland and Antarctic ice sheets. *Nature* **461,** 971–975 (2009).
3. Wingham, D. J., Wallis, D. W. & Shepherd, A. Spatial and temporal evolution of Pine Island Glacier thinning, 1995–2006. *Geophys. Res. Lett.* **36,** L17501 (2009).
4. Rignot, E., Velicogna, I., van den Broeke, M. R., Monaghan, A. & Lenaerts, J. Acceleration of the contribution of the Greenland and Antarctic ice sheets to sea level rise. *Geophys. Res. Lett.* **38,** L05503 (2011).
5. Jacobs, S. S., Jenkins, A., Giulivi, C. F. & Dutrieux, P. Stronger ocean circulation and increased melting under Pine Island Glacier ice shelf. *Nature Geosci.* **4,** 519–523 (2011).
6. Ó Cofaigh, C. *et al.* Flow of the West Antarctic Ice Sheet on the continental margin of the Bellingshausen Sea at the Last Glacial Maximum. *J. Geophys. Res.* **110,** B11103 (2005).
7. Holland, P. R., Jenkins, A. & Holland, D. M. Ice and ocean processes in the Bellingshausen Sea, Antarctica. *J. Geophys. Res.* **115,** C05020 (2010).
8. Chen, J. L., Wilson, C. R., Blankenship, D. & Tapley, B. D. Accelerated Antarctic ice loss from satellite gravity measurements. *Nature Geosci.* **2,** 859–862 (2009).
9. Schoof, C. Ice sheet grounding line dynamics: steady states, stability, and hysteresis. *J. Geophys. Res.* **112,** F03S28 (2007).
10. Blankenship, D. D. *et al.* in *The West Antarctic Ice Sheet: Behaviour and Environment* (eds Alley, R. B. & Bindschadler, R. A.) *Antarct. Res. Ser.*, **77,** 105–121 (AGU, 2001).
11. Winberry, J. P. & Anandakrishnan, S. Crustal structure of the West Antarctic Rift System and Marie Byrd Land hotpsot. *Geology* **32,** 977–980 (2004).
12. Dalziel, I. W. D. On the extent of the active West Antarctic Rift System. *Terra Antarctica Rep.* **12,** 193–202 (2006).
13. Anandakrishnan, S., Blankenship, D. D., Alley, R. B. & Stoffa, P. L. Influence of subglacial geology on the position of a West Antarctic ice stream from seismic observations. *Nature* **394,** 62–65 (1998).
14. Studinger, M. *et al.* Subglacial sediments: a regional geological template for ice flow in West Antarctica. *Geophys. Res. Lett.* **28,** 3493–3496 (2001).
15. Maule, C. F., Purucker, M. E., Olsen, N. & Mosegard, K. Heat flux anomalies in Antarctica revealed by satellite magnetic data. *Science* **309,** 464–467 (2005).
16. Müller, R. D., Gohl, K., Cande, S. C., Goncharov, A. & Golynsky, A. V. Eocene to Miocene geometry of the West Antarctic Rift System. *Aust. J. Earth Sci.* **54,** 1033–1045 (2007).
17. LeMasurier, W. E. Neogene extension and basin overdeepening in the West Antarctic rift inferred from comparisons with the East African rift and other analogs. *Geology* **36,** 247–250 (2008).
18. Harbor, J. M. Numerical modeling of the development of U-shaped valleys by glacial erosion. *Geol. Soc. Am. Bull.* **104,** 1364–1375 (1992).
19. Olsen, K. H. & Morgan, P. in *Continental Rifts: Evolution, Structure, Tectonics* (ed. Olsen, K. H.) 3–26 (Elsevier, 2006).
20. Maslanyj, M. P. & Storey, B. C. Regional aeromagnetic anomalies in Ellsworth Land: crustal structure and Mesozoic microplate boundaries within West Antarctica. *Tectonics* **9,** 1515–1532 (1990).
21. Siddoway, C. S. in *Antarctica: a Keystone in a Changing World* (eds Cooper, A. K. *et al.*), *Proc. 10th Int. Symp. Ant. Sci.* 91–114 (The National Academies Press, 2008).
22. Gohl, K. Basement control on past ice sheet dynamics in the Amundsen Sea Embayment, West Antarctica. *Palaeogeogr. Palaeoclim. Palaeoecol.* **335/ 6,** 35–41 (2012).
23. Jordan, T. A. *et al.* Aerogravity evidence for major crustal thinning under the Pine Island Glacier region (West Antarctica). *Geol. Soc. Am. Bull.* **122,** 714–726 (2010).
24. Granot, R., Cande, S. C., Stock, J. M., Davey, F. J. & Clayton, R. W. Postspreading rifting in the Adare Basin, Antarctica: regional tectonic consequences. *Geochem. Geophys. Geosyst.* **11,** Q08005 (2010).
25. Schröder, H., Paulsen, T. & Wonik, T. Thermal properties of the AND-2A borehole in the southern Victoria Land Basin, McMurdo Sound, Antarctica. *Geosphere* **7,** 1324–1330 (2011).
26. Taylor, J. *et al.* Topographic controls on post-Oligocene changes in ice-sheet dynamics, Prydz Bay region, East Antarctica. *Geology* **32,** 197–200 (2004).
27. De Angelis, H. & Kleman, J. Palaeo-ice streams in the Foxe/Baffin sector of the Laurentide Ice Sheet. *Quat. Sci. Rev.* **26,** 1313–1331 (2007).
28. Rignot, E. *et al.* Recent Antarctic ice mass loss from radar interferometry and regional climate modelling. *Nature Geosci.* **1,** 106–110 (2008).
29. Vaughan, D. G. *et al.* New boundary conditions for the West Antarctic ice sheet: subglacial topography beneath Pine Island Glacier. *Geophys. Res. Lett.* **33,** L09501 (2006).
30. Graham, A. G. C., Nitsche, F. O. & Larter, R. D. An improved bathymetry compilation for the Bellingshausen Sea, Antarctica, to inform ice-sheet and ocean models. *Cryosphere* **5,** 95–106 (2011).

Supplementary Information is linked to the online version of the paper at www.nature.com/nature.

Acknowledgements This study was supported by the Natural Environment Research Council (NERC/AFI/CGS/11/60) and British Antarctic Survey research programme Polar Science for Planet Earth. We acknowledge NASA Operation IceBridge for airborne ice-sounding data, A. G. C. Graham for bathymetry data and C. Griffiths for field assistance.

Author Contributions All authors contributed to research design. R.G.B. performed the field research. R.G.B. and E.C.K. processed radar data. F.F. analysed and interpreted the aeromagnetic and aerogravity data; all authors participated in data discussion and interpretation; R.G.B. and F.F. wrote the manuscript; and all authors contributed substantial comments and editorial revisions.

Author Information Reprints and permissions information is available at www.nature.com/reprints. The authors declare no competing financial interests. Readers are welcome to comment on the online version of this article at www.nature.com/nature. Correspondence and requests for materials should be addressed to R.G.B. (r.bingham@abdn.ac.uk).

doi:10.1038/nature11292

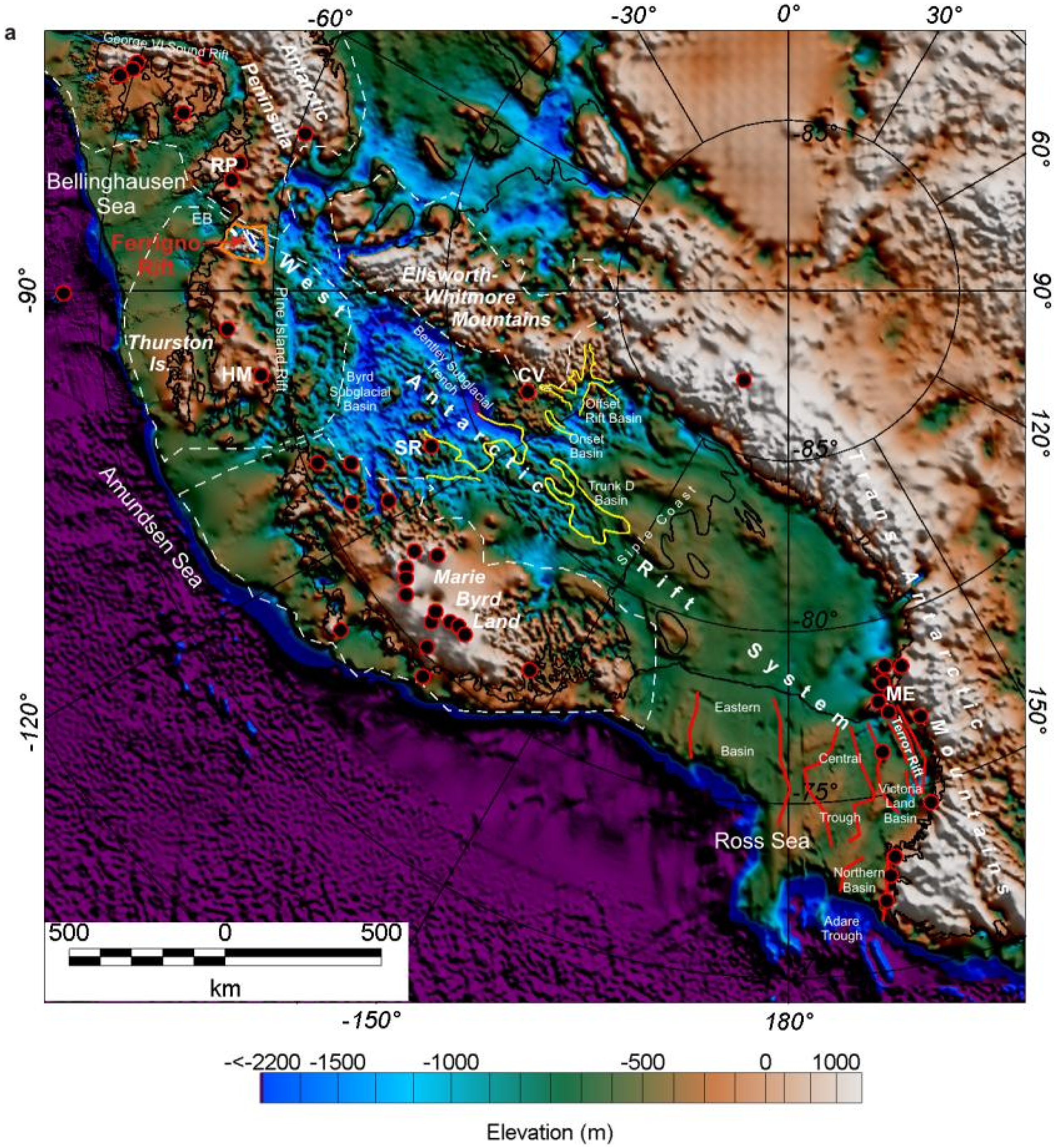

Supplementary Figure 1. Geophysical perspectives of the West Antarctic Rift System.

a, **Topography of the West Antarctic Rift System.**

This new map was obtained by combining our bedrock topography grid over the Ferrigno Rift with recent swath bathymetry data over the adjacent Bellingshausen Sea[30] and with previous radar and bathymetry data for the Amundsen and Ross Sea sectors of West Antarctica[29,31]. The orange line outlines the Ferrigno glacial catchment.

Note that despite its potential influence on WAIS dynamics, the West Antarctic Rift System (WARS) remains the most poorly understood continental rift system on Earth[32]. Only the Ross Sea segment of the rift system has relatively more comprehensive geophysical data coverage, including seismic reflection and refraction data[33,34], gravity[35-37] and magnetic data[38-40]; and it includes several drill sites that help constrain Cretaceous and Cenozoic tectonic evolution within the WARS[e.g. 41,42]. Although the size and evolution of the WARS have been compared to active rift systems, such as the Basin and Range Province in the US and the East African Rift System, the extent of its active or recently active portions remains conjectural[12]. Large sectors of the WARS are likely to be either inactive or dormant, based on the low level of seismicity[43], magnetotelluric data[44] and GPS measurements[45].

The red lines show Cretaceous-Cenozoic rift basins that contain several km thick sedimentary infill over the Ross Sea region[33,46]. The yellow lines indicate major sedimentary basins in the interior of the WARS that have been delineated from aeromagnetic data analysis[47], using depth to magnetic source estimate techniques[48] similar to those used in our study (see Figure 3c & Supplementary Figure 8). These sedimentary basins have been interpreted as a key geological template that facilitates fast glacial flow for the Siple Coast ice streams[10,13-14].

The black circles with a red outline denote Cenozoic volcanoes associated with the WARS[49]. Mount Erebus (ME) is a major active volcano. Other active or recently active volcanoes that have been inferred from geophysical interpretations to influence the overlying West Antarctic Ice Sheet (WAIS) include Casertz Volcano (CV)[50], the Hudson Mountains volcano (HM)[51], and a proposed caldera complex along the Sinuous Ridge (SR)[52].

The white dashed lines indicate the four major crustal blocks of West Antarctica, which include the Antarctic Peninsula, the Thurston Island-Eights Coast crustal block, the Ellsworth-Whitmore crustal block, and the Marie Byrd Land crustal block[53].

We propose that the Ferrigno Rift (white solid lines) is located along the northeastern extension of the WARS[16]. Finite rotation poles that have been calculated for WARS extension are not local to West Antarctica, which requires the rift system to have connected to other plate boundaries at both ends[54]. A link through the George VI Sound Rift[55,56] could have connected the WARS to the subduction trench that was active along the western margin of the Antarctic Peninsula during most of the Cenozoic (see Ref. 54 for post-35 Ma reconstructions of the evolution of the trench). It appears likely that the newly identified Ferrigno Rift exploited the pre-existing crustal boundary between the Antarctic Peninsula and Thurston Island-Eights Coast blocks.

Movements of these crustal blocks relative to each other and East Antarctica may have occurred as early as Middle to Late Jurassic times (~180-140 Ma), possibly triggering the earliest phases of extension and/or strike slip motion within West Antarctica[12]. This was followed by widespread Cretaceous intracontinental extension across the Ross Sea and central West Antarctica[21]. Geological studies over Marie Byrd Land suggest that a major phase of WARS extension occurred in a dextral transcurrent regime between 105-90 Ma, and was linked to oblique convergence along the active paleo-Pacific margin of West Antarctica[21].

Cenozoic reactivation of the WARS is evident within the Victoria Land Basin and the Northern Basin in the Ross Sea[57]; this rifting stage has been related to sea-floor spreading in the Adare Trough, where up to 180 km of extension between East and West Antarctica occurred between 46-21 Ma[58]. Neogene reactivation of the WARS occurred within the narrow Terror Rift in the western Ross Sea[59]. This phase of extension may relate to post-spreading rifting recently identified in the Adare Basin. Although the extent of Neogene rifting in the interior of the WARS remains poorly constrained, recent studies suggest that both the Bentley Subglacial Trench and Byrd Subglacial Basin were affected by Neogene extension[17].

doi:10.1038/nature11292

We hypothesise that Neogene reactivation occurred also in the Ferrigno Rift and Pine Island Rift regions, potentially causing enhanced geothermal heat flux that would increase the availability of meltwater at the base of the WAIS. Overall, we propose that these narrow and glacially over-deepened rift basins exert a key influence on the WAIS, by effectively steering ongoing dynamic thinning processes further inland.

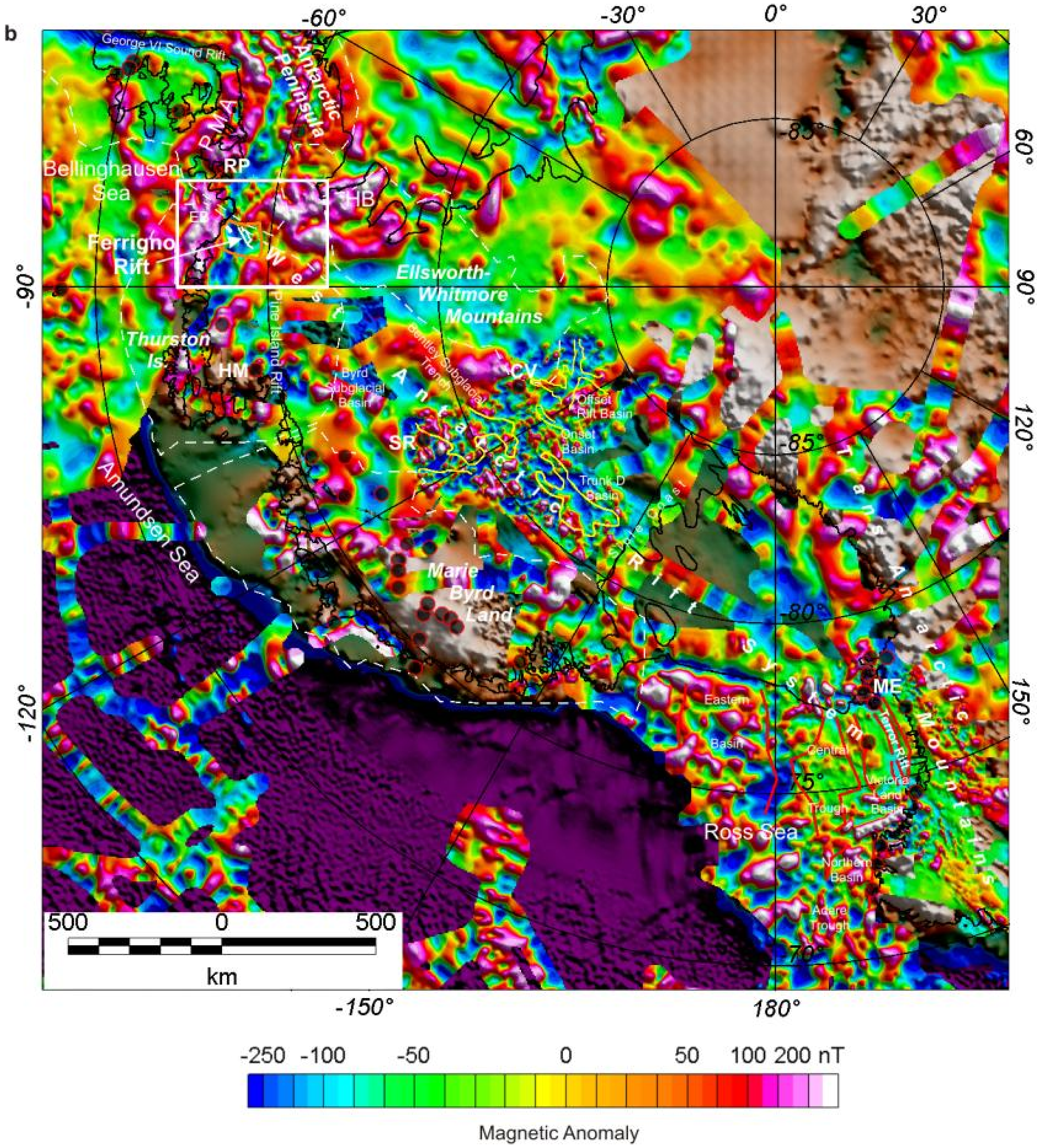

b, **Magnetic anomaly map of the West Antarctic Rift System.**

The map was compiled by combining magnetic data from a variety of sources: i) aeromagnetic data over the western part of the Ross Sea Rift that were collected during GANOVEX surveys[60]; ii) GITARA & GANOVEX aeromagnetic data over Marie Byrd Land and the Transantarctic Mountains[40,61]; ii) CASERTZ-SOAR data over

Central West Antarctica[62]; iv) SPARC aeromagnetic data over the Antarctic Peninsula[54]; and a variety of older aeromagnetic and marine magnetic data that were combined within the ADMAP project[63].

We also reprocessed reconnaissance aeromagnetic data for our study area[20] (white rectangle) to provide regional coverage for the catchment of Ferrigno Ice Stream (orange outline as in Supplementary Figure 1a). The location of flight lines for our study area is displayed in Supplementary Figure 5a, and more detailed views of the aeromagnetic data are shown in Supplementary Figures 6a-b.

Note that aeromagnetic anomalies provide a key geophysical tool for imaging the subglacial and submarine extent of rift-related magmatism in the WARS[64]. The linear rift fabric is particularly evident over the Ross Sea part of the WARS[38] . The magnetic signatures reflect Cenozoic volcanism emplaced along rift faults, some of which were likely reactivated during regional Cenozoic extension and/or strike-slip faulting[32,40]. Several high amplitude circular anomalies lie at high angle to the rift basins and reveal the extent of major Cenozoic alkaline intrusions. These intrusions have been interpreted as being emplaced along transfer faults that link major rift basins[57].

In central West Antarctica, linear rift fabric is less evident from magnetic signatures. High-amplitude and more circular magnetic anomalies are interpreted as reflecting widespread Cenozoic magmatism beneath WAIS[65]. Here, the majority of magnetic anomalies lack a distinct topographic expression, suggesting that most volcanic edifices were eroded by fast moving ice associated with the Siple Coast ice streams. The anomalies are interpreted as caused by several-km thick sub-volcanic mafic intrusions of inferred late Cenozoic age[65]. However, the proposed late Cenozoic age for these intrusions and associated eroded volcanoes has been questioned, because of the paucity of late Cenozoic mafic volcanic debris recovered at the base of several West Antarctic ice cores[66].

Cenozoic magmatism may potentially be longer-lived, as is observed over the Transantarctic Mountains that flank the WARS[67]. For some magnetic anomalies, such as the Casertz Volcano (CV), a drawdown of the ice-sheet surface is also observed[50]. This suggests the occurrence of active or recently active volcanism and locally highly elevated geothermal heat flux[50]. Elevated geothermal flux from subglacial volcanism and associated intrusions could have significant effects on sub-ice hydrology and ice flow dynamics[68].

In the Ferrigno catchment area, we found no evidence from widely spaced aeromagnetic data for high-amplitude magnetic anomalies typically attributed to large Cenozoic intrusions and major volcanic provinces in other sectors of the WARS. A comparison between magnetic anomaly patterns over the Pine Island Glacier catchment (See Supplementary Figure 11) and the Ferrigno catchment suggests that the northeastern extension of the WARS is likely to be more weakly magmatic compared to the interior of the rift system. We note, however, that there are some exposures of Cenozoic volcanic rocks in both the Thurtson Island block and east of Eltanin Bay (EB) in the Ryberg Peninsula[49] (RP). There was some volcanic activity in the latter area as recently as the Pliocene[69]. Furthermore, it has been proposed that the entire region from Marie Byrd Land to the Antarctic Peninsula is a part of a larger Cenozoic diffuse alkaline magmatic province[70]. Therefore, the possibility of more localised Neogene to recent magmatic activity within the Ferrigno Rift region cannot be dismissed without higher resolution magnetic surveys (e.g. see Ref. 40 for aeromagnetic studies that have revealed localised Cenozoic volcanism over the Transantarctic Mountains).

Note that major magnetic anomalies in the Ferrigno catchment region include a long-wavelength magnetic high that is part of the Pacific Margin Anomaly (PMA), which is attributed to a Mesozoic magmatic arc[e.g.55], and to the southeast magnetic highs reveal the extent of the Precambrian Haag Block (HB). See Supplementary Figure 6a for further explanation.

doi:10.1038/nature11292

c, Estimates of crustal thickness for the West Antarctic Rift System between the Amundsen and Bellingshausen sea region.

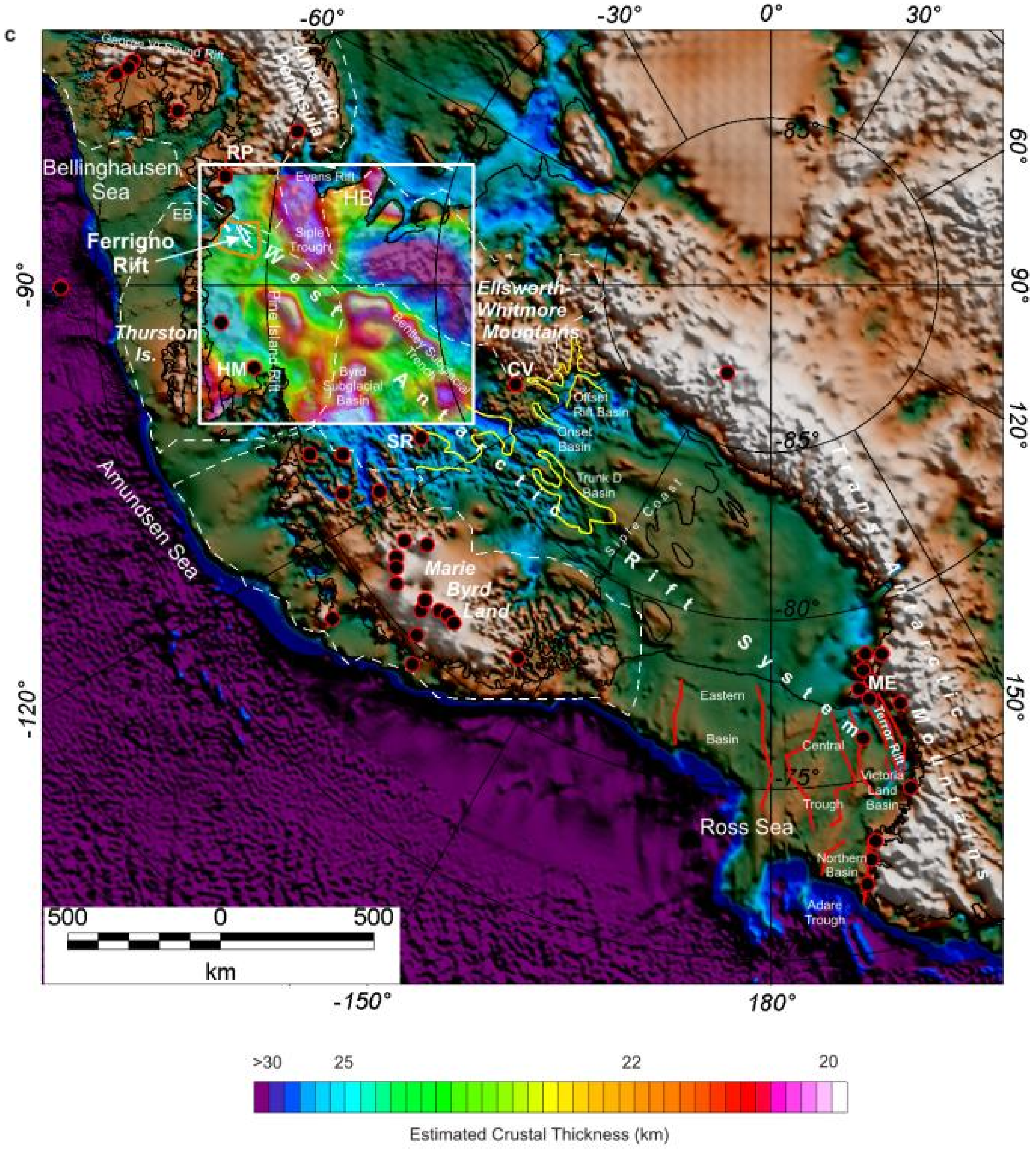

The new crustal thickness map for the proposed northeasterly extension of the WARS (white rectangle) was obtained from inversion of combined GRACE (Gravity Recovery and Climate Experiment) and GOCE (Gravity Field and Steady State Ocean Circulation Explorer) satellite gravity data using the global gravity model *GOCO01S* downloaded from http://icgem.gfz-potsdam.de/ICGEM/ICGEM.html and from recent airborne gravity data[23]. A larger scale view of the crustal thickness map is shown in Supplementary Figure 10.

Note that the satellite gravity field model is resolved up to degree/order 224 of a harmonic series expansion corresponding to a half-wavelength of ~100 km. Hence narrow regions of thinned crust that are likely to underlie the Ferrigno Rift are not resolved from satellite gravity data inversion. We also note that the only seismic constraint to tie our gravity inversion results beneath this part of WAIS derives from the Bentley Subglacial Trench region, where a single estimate of crustal thickness derives from receiver functions[71].

We used GM-SYS 3D to estimate crustal thickness using Parker inversion applied to Bouguer gravity anomaly data, following the methodology recently used in East Antarctica to investigate crustal thickness within the East Antarctic Rift System and the adjacent Gamburtsev Subglacial Mountains[72]. Our starting model assumed a 35 km reference crustal thickness and a density contrast between the crust and mantle interface of 400 kg m^{-3}.

Our estimates are in general agreement with previous inversions of airborne gravity data derived from other methods (e.g. terrain de-correlated Free-Air anomalies) over the Pine Island Glacier region[23]. We also compared our gravity-derived crustal thickness estimates with independent results derived from 3D flexural modelling of subglacial topography (see e.g. ref. 72 for similar methods recently applied in East Antarctica), and noted a good agreement, provided relatively low values of elastic thickness are assumed for the WARS (0<Te<30 km) (see also ref. 23). We also found a good agreement between our regional crustal thickness estimates onshore and independent estimates derived offshore in the Amundsen Sea from wide-angle seismic data[22,73].

The new map clearly images thinner crust beneath the Pine Island Rift, Byrd Subglacial Basin, Bentley Subglacial Trench, and also under the Siple Trough and Evans Rift[74] region. The 20-25 km thick crust we imaged provides new geophysical evidence for an extension of the WARS under the Amundsen and Bellingshausen sectors of WAIS.

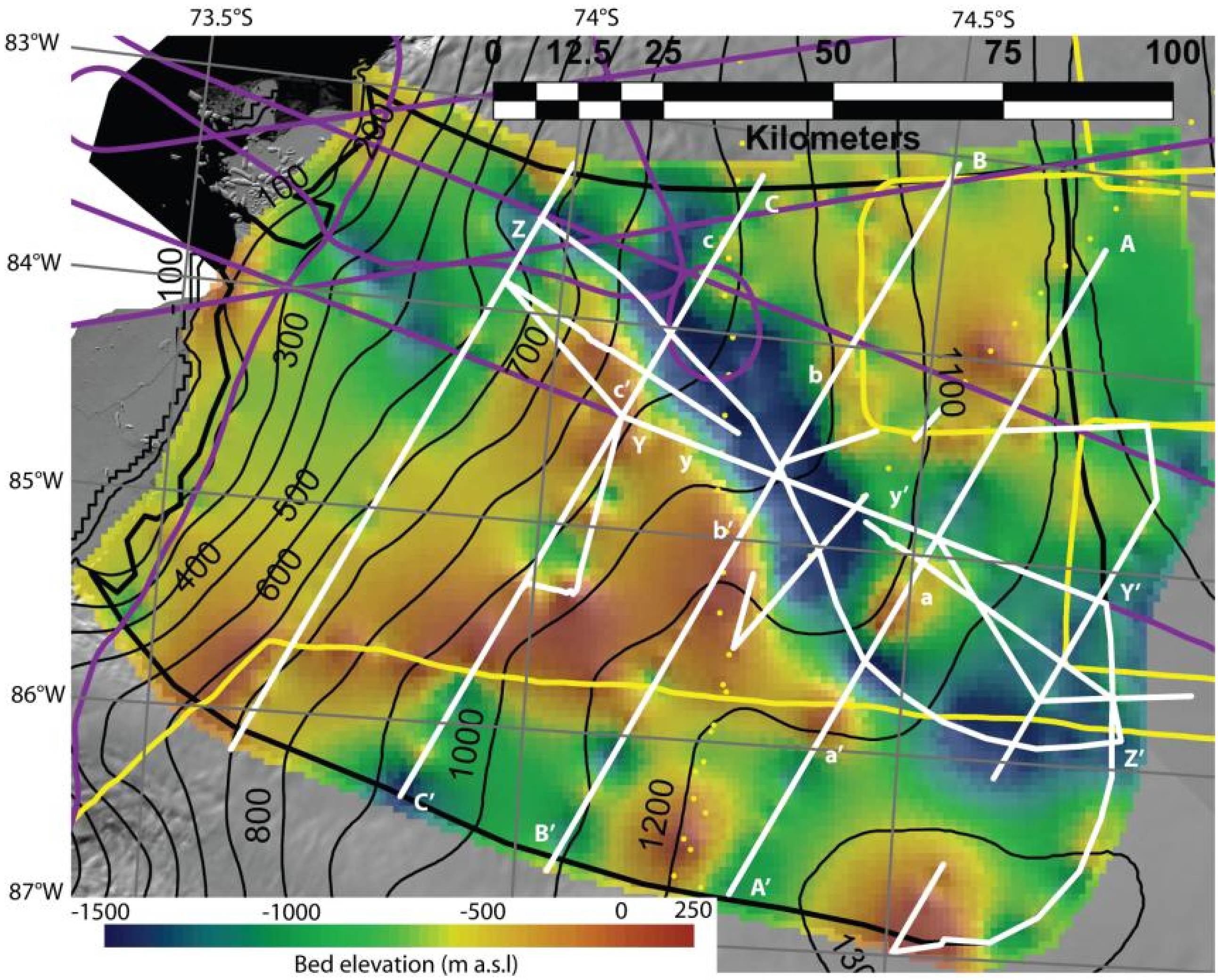

Supplementary Figure 2. Large-scale figure of Ferrigno Ice Stream basal topography with 2009/10 radar profiles superimposed. DELORES radar profiles are shown in white, with labels referring to profiles shown in Supplementary Figure 3 (e.g. AA') and Supplementary Figure 4 (e.g. aa'). Purple lines show NASA MCoRDS radar tracks from 3 November 2009; yellow tracks pre-existing bed data. Also shown: catchment boundary (black polygon); 100 m ice surface contours (thin black lines).

Supplementary Figure 3 (overleaf). Additional radar profiles showing morphology of Ferrigno Ice Stream bed. Locations of profiles marked in Supplementary Figure 2. Profile AA' is a repeat of that shown in Fig. 2a; profiles BB' and CC' are parallel profiles 25 and 50 km downstream respectively. Profile YY' trends NW-SE, almost orthogonal to AA', BB' and CC' but also traversing the rift. In each profile, distance is given relative to the rift centre-line (path followed by profile ZZ'). Green boxes locate close-ups across rift detailed in Supplementary Figure 4.

In interpreting these profiles, some artefacts must be noted and discounted from geological interpretation as follows: (i) BB' 15-30 km: interference rising from the bottom-to-centre of image was introduced by a battery-regulator erroneously left on during radar acquisition; (ii) CC' 18-26 km: signal suppression due to overheating; (iii) sporadic vertical lines in all profiles: occasional breaks in signal resulting from sporadic transmitter overheats.

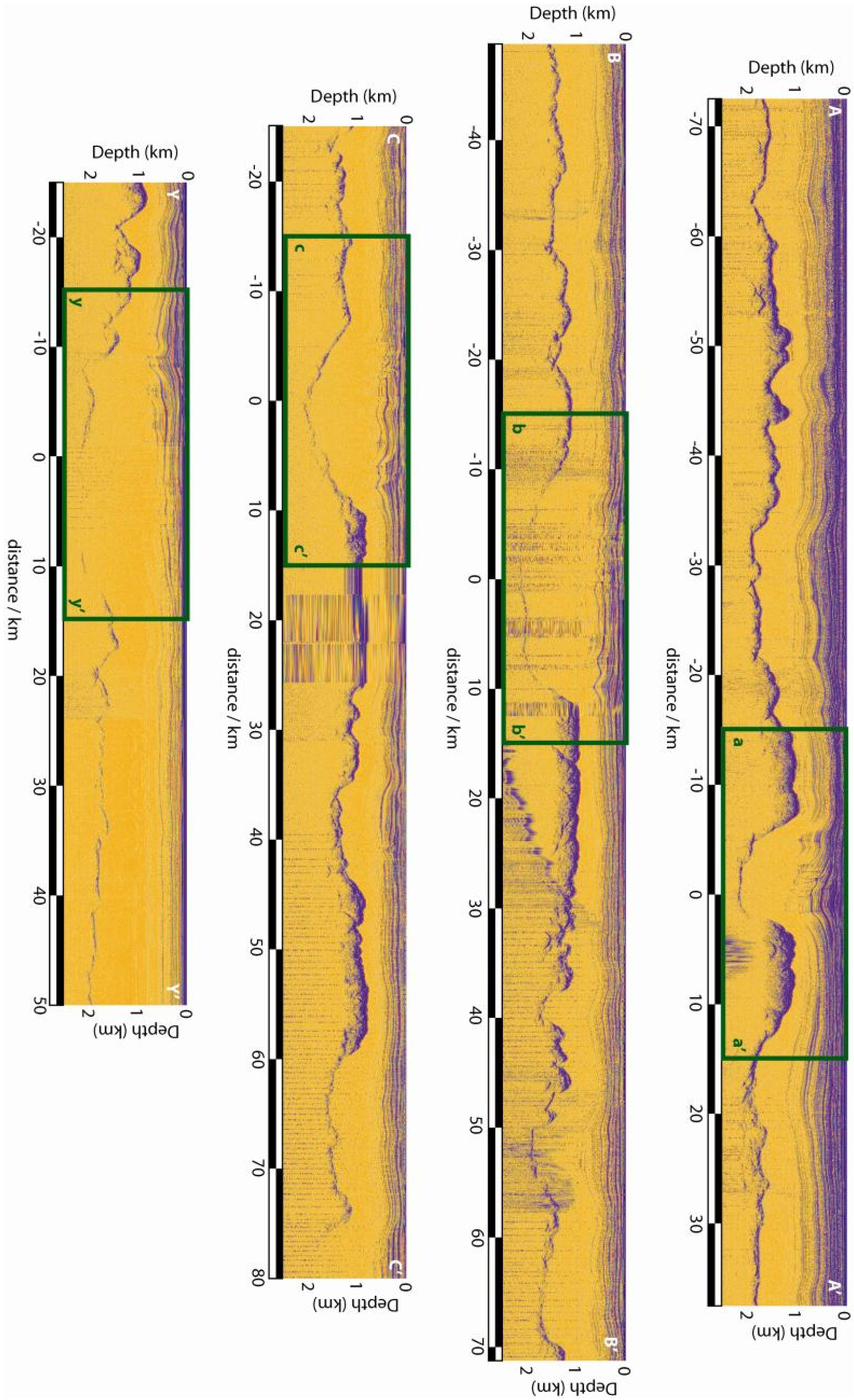
Depth (km)
distance / km
A
A′
a
a′
B
B′
b
b′
C
C′
c
c′
Y
Y′
y
y′

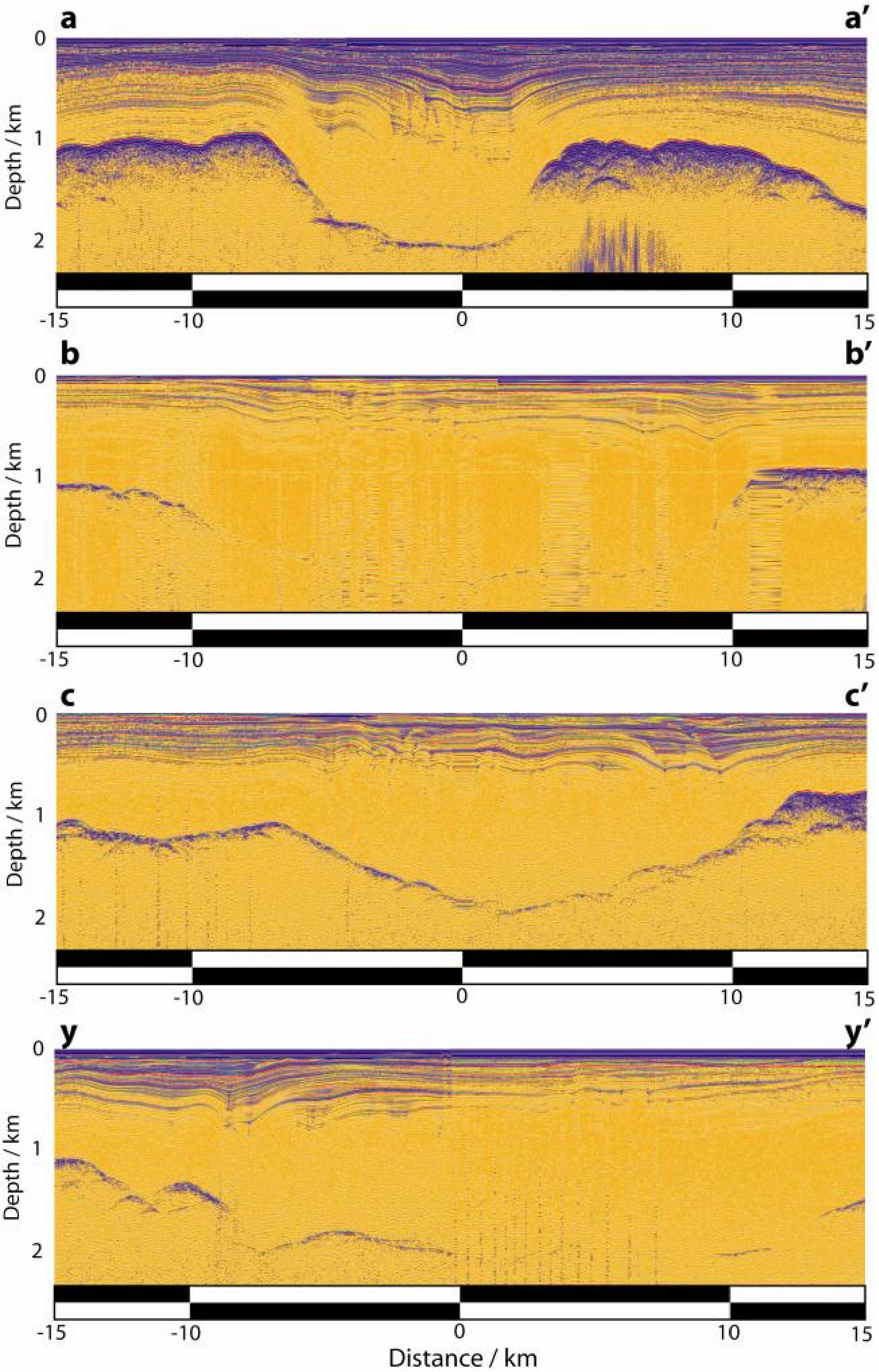

Supplementary Figure 4. 30 km radar profiles traversing rift. Subsets of profiles shown in Supplementary Figure 3; locations of profiles marked in Supplementary Figure 2.

doi:10.1038/nature11292

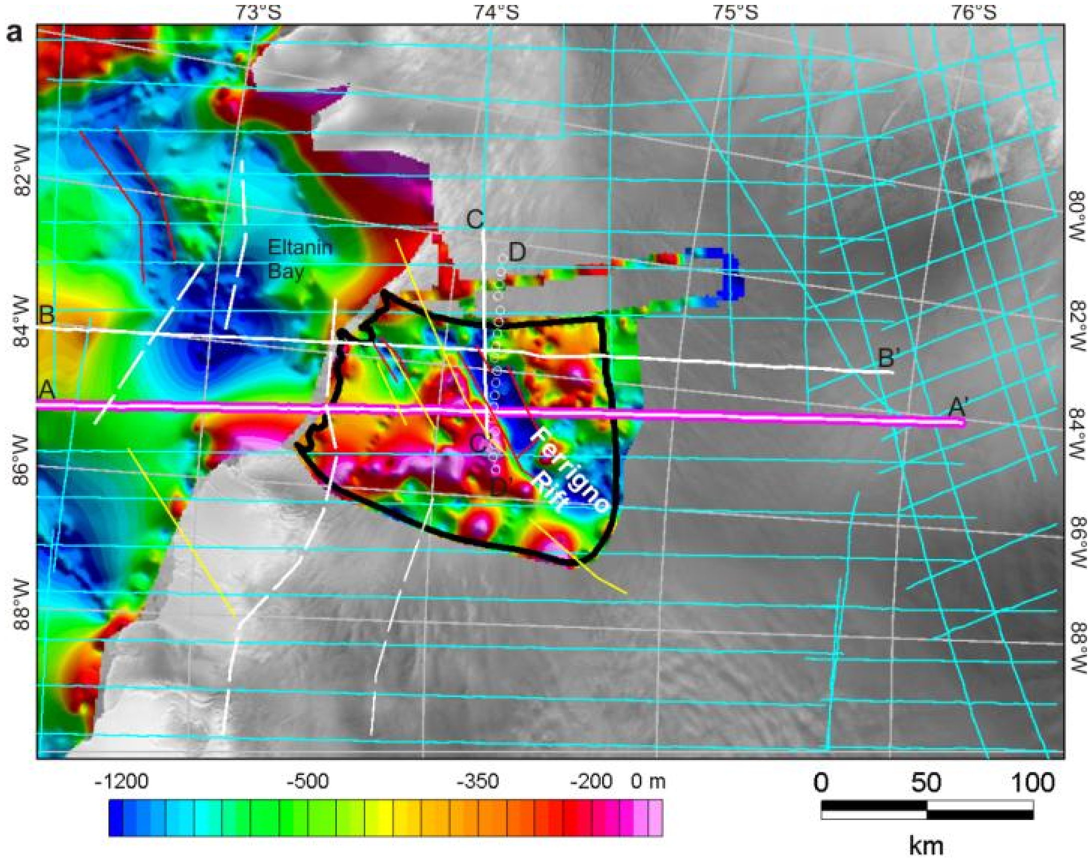

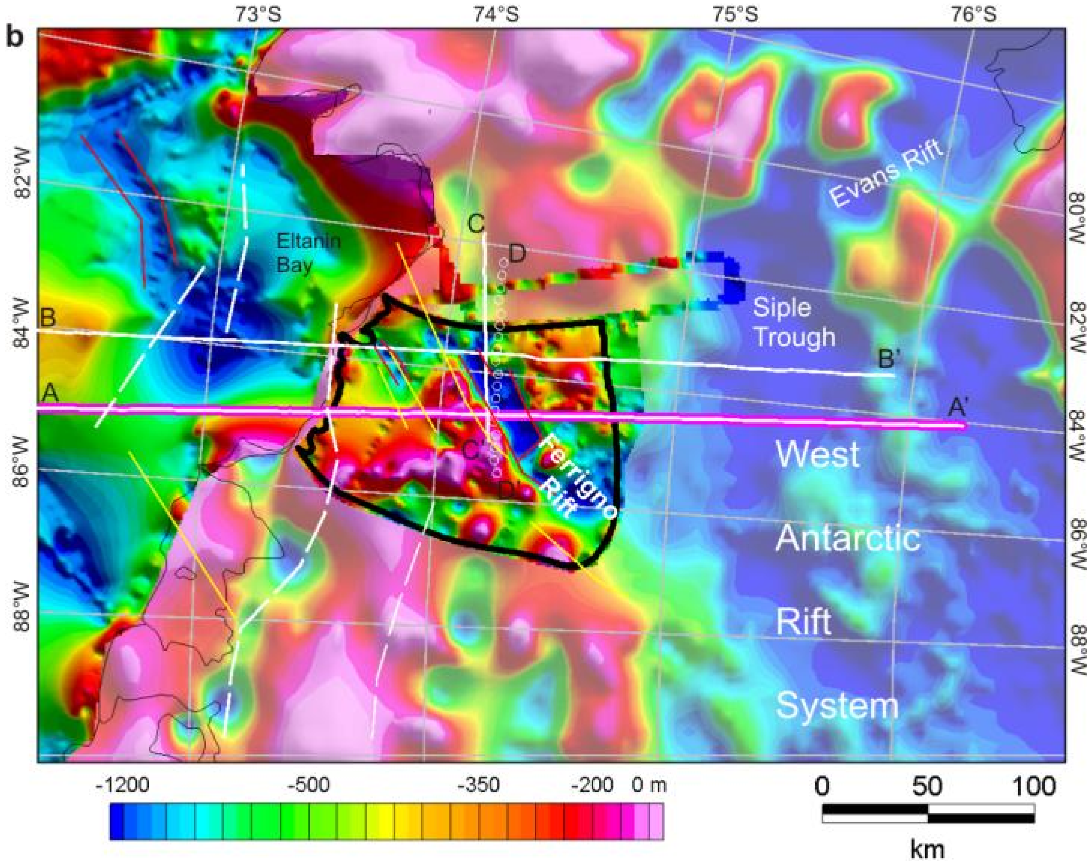

Supplementary Figure 5. Aeromagnetic flight lines and location of gravity and magnetic models for the Ferrigno Rift region.

Supplementary Figure 5 a, Aeromagnetic lines for the Ferrigno catchment (black outline) are shown in blue[20] and are overlain on a digital elevation model of WAIS from the RADARSAT-1 Antarctic Mapping Project (RAMP) (http://bprc.osu.edu/rsl/radarsat/data/). Offshore we included recent swath bathymetry data over the Eltanin Bay region[30].

Note that the flight line spacing is ca. 20 to 30 km. This is coarse, when compared to the ca. 5 km line spacing available for the Ross Sea Rift[60] and over parts of Marie Byrd Land[61] and central West Antarctica[62].

The red lines denote the inferred Ferrigno Rift, which we interpret as including a series of northeast-southwest oriented left-stepping en-echelon segments. The white dashed lines denote the location of magnetic lineaments that we associate with the Pacific Margin Anomaly and adjacent Thurston Island Province. The yellow lines denote magnetic lineaments that we interpret as related to rifting (see Supplementary Figure 6). AA', BB', CC' and DD' denote the locations of our magnetic and gravity models. The white circles show the locations of land-gravity measurements used in our study.

b, Locations of our magnetic and gravity models superimposed on subglacial topography for the West Antarctic Rift System. Symbology and lettering follow panel a. Note that the newly identified Ferrigno Rift is roughly parallel to the broader subglacial rift basins identified further in the interior of the WARS (e.g. the Siple Trough that can now be inferred to connect to the previously recognised Evans Rift[74]).

Supplementary Figure 6 (overleaf). Aeromagnetic anomaly maps for the northeastern segment of the West Antarctic Rift System, including the Ferrigno Rift.

a, Total field magnetic anomaly map. The map was derived by re-processing aeromagnetic data collected during the 1986-87 field season over West Antarctica[20]. The data were re-levelled using statistical levelling techniques and residual flight-line noise was further reduced by applying microlevelling in the frequency domain[75]. These procedures enabled us to reduce cross-over errors to <5 nT. The microlevelled data were then gridded on a 5 km mesh and were draped onto our new bedrock topography digital elevation model at a distance of 3,500 m from the bed (corresponding to the mean distance between the aircraft and the bed).

The map shows a linear, ~coast-parallel and predominantly positive magnetic anomaly that is part of the major magnetic anomaly belt that extends from the Antarctic Peninsula to Thurston Island - known as the Pacific Margin Anomaly[e.g. 55] (see also Supp. Fig. 1b). It is flanked to the south by a broad negative anomaly that forms the more weakly magnetic Thurston Island Province. This broad magnetic low is punctuated by high-frequency magnetic highs with amplitudes of ~100 nT and wavelengths of ca. 20 km. We interpret this region as forming the back-arc region of main Mesozoic magmatic arc. A linear northeast trending magnetic low is interpreted as reflecting the magnetic signature of the weakly magnetic rifted crust associated with the Ferrigno Rift. Further to the south a broad positive magnetic anomaly pattern with amplitudes above 400 nT delineates the extent of the Precambrian Haag Province, which we interpret here as forming a major basement horst lying between the Siple Trough and Evans Rift region. To the southwest of the Ferrigno catchment, we identify several high-amplitude magnetic highs that we interpret as revealing the extent of more widespread Cenozoic magmatism further in the interior of the West Antarctic Rift System.

b, Tilt derivative magnetic anomaly map for the Ferrigno catchment. To enhance linear magnetic anomalies and help detect the edges of the sources of the magnetic bodies we computed the tilt derivative map for the catchment of Ferrigno Ice Stream (black outline). A description of tilt derivative methods is reported in Ref. 76. The tilt derivative map enhances shallow-source magnetic anomalies and clearly images the linear magnetic low associated with the Ferrigno Rift region (compare yellow lines showing magnetic lineaments & red lines showing the interpreted en echelon rift basins). The map also helps to locate the intrusions that we interpreted in the back-arc region.

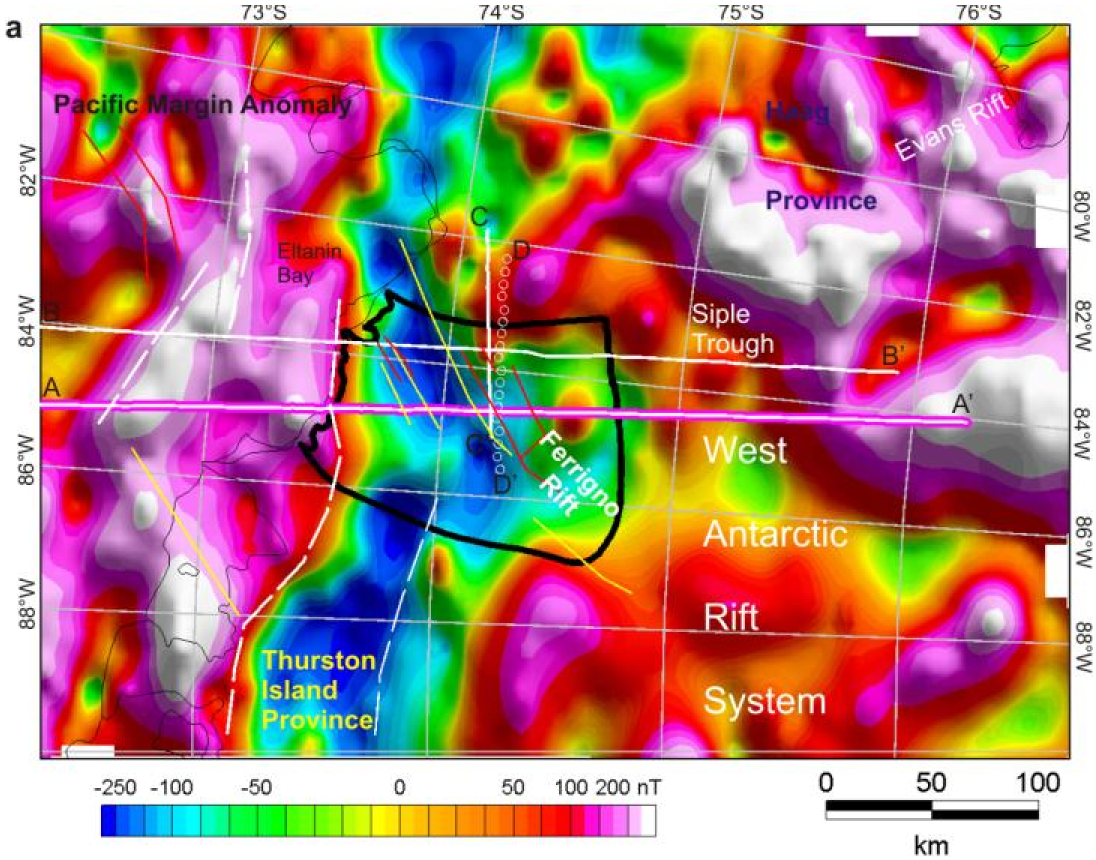

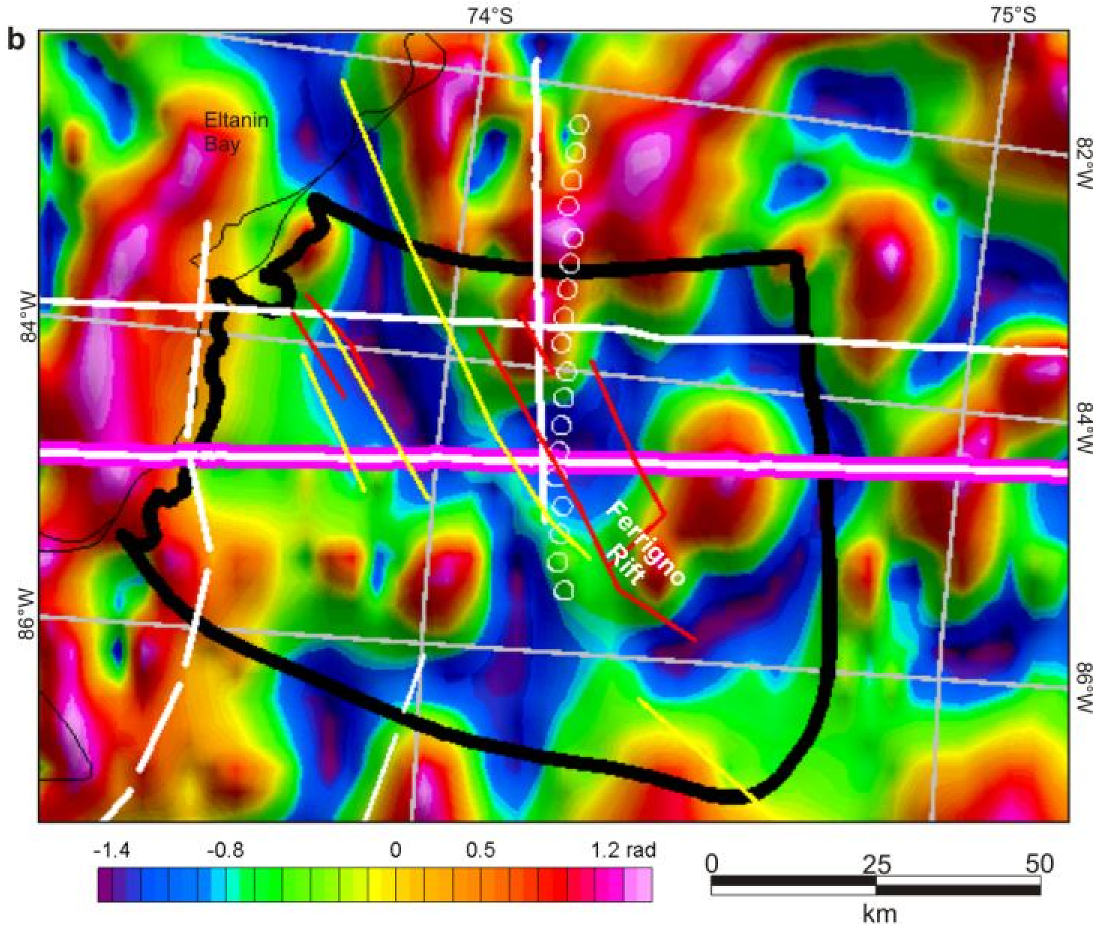

Supplementary Figure 6 (full caption on previous page).

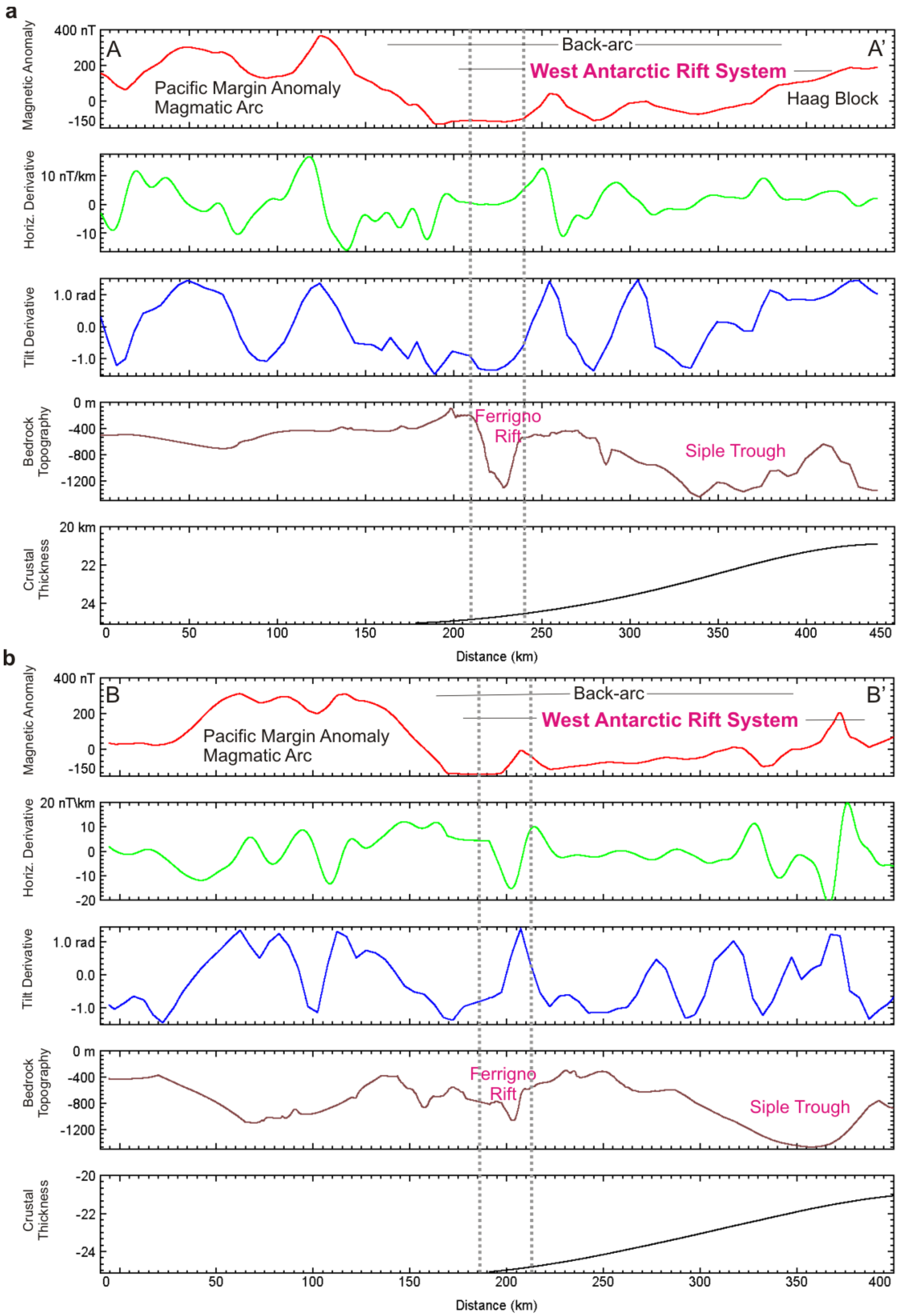

Supplementary Figure 7, parts a and b. Caption for these figures on following page.

doi:10.1038/nature11292

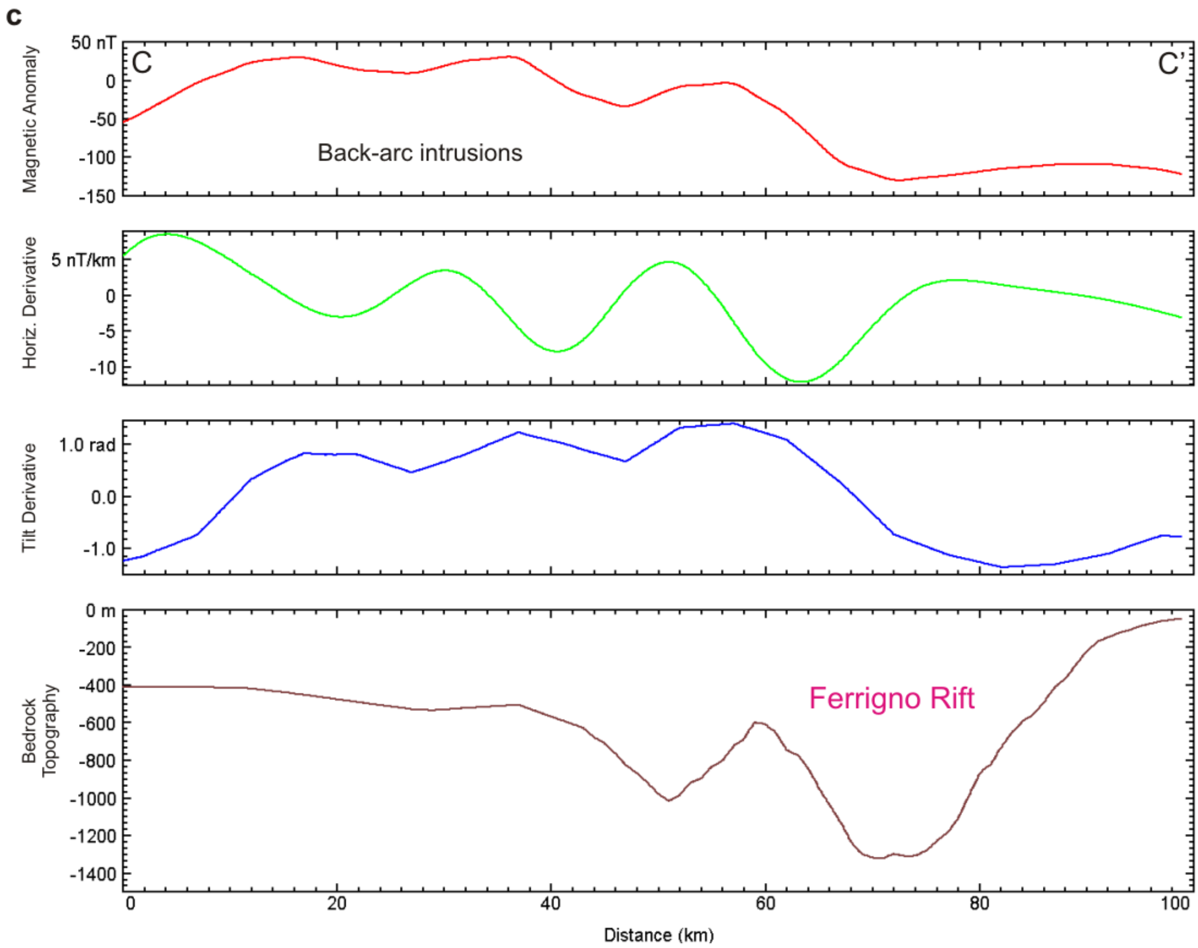

Supplementary Figure 7. Profile views of magnetic anomaly, topography and crustal thickness for the northeastern segment of the West Antarctic Rift System, including the Ferrigno Rift.

a, Profile view along section A-A' (see Supp. Figs. 5 and 6 for location). The upper panel shows the total field magnetic anomalies. In the north, long-wavelength anomalies are characteristic of the Pacific Margin Anomaly, which reflects the Mesozoic magmatic arc; further south a broad magnetic low is interpreted as reflecting the West Antarctic Rift System that developed primarily within the back-arc region.

To enhance the edges of the magnetic anomalies and shallower source bodies we calculated both the horizontal derivative and tilt derivative anomalies[73]. Note the quiet magnetic signature of the horizontal derivative and tilt derivative over the Ferrigno Rift region and the sharp peaks along its southern edge. Prominent peaks are seen also over the interpreted back-arc intrusions (see also Supp. Fig. 6b). The quiet magnetic signature detected from the derivatives suggests a dearth of shallow sources over the Ferrigno Rift region, which is consistent with our interpretation of sedimentary infill within the rift basin. (see also Supp. Fig. 8).

b, Profile view along section B-B'. In this section the Ferrigno Rift is not as deep and is narrower and the derivatives suggest the existence of a shallow intrusion along its southern flank.

c, Profile view along section C-C'. This ~E-W oriented section shows the sharp western boundary of the Ferrigno Rift, with the total field and derivative magnetic data suggesting the occurrence of intrusions along its flank. This section is the closest to the line that includes gravity measurements (see Supplementary Figure 6 for location) and that is shown in Figure 3d.

doi:10.1038/nature11292

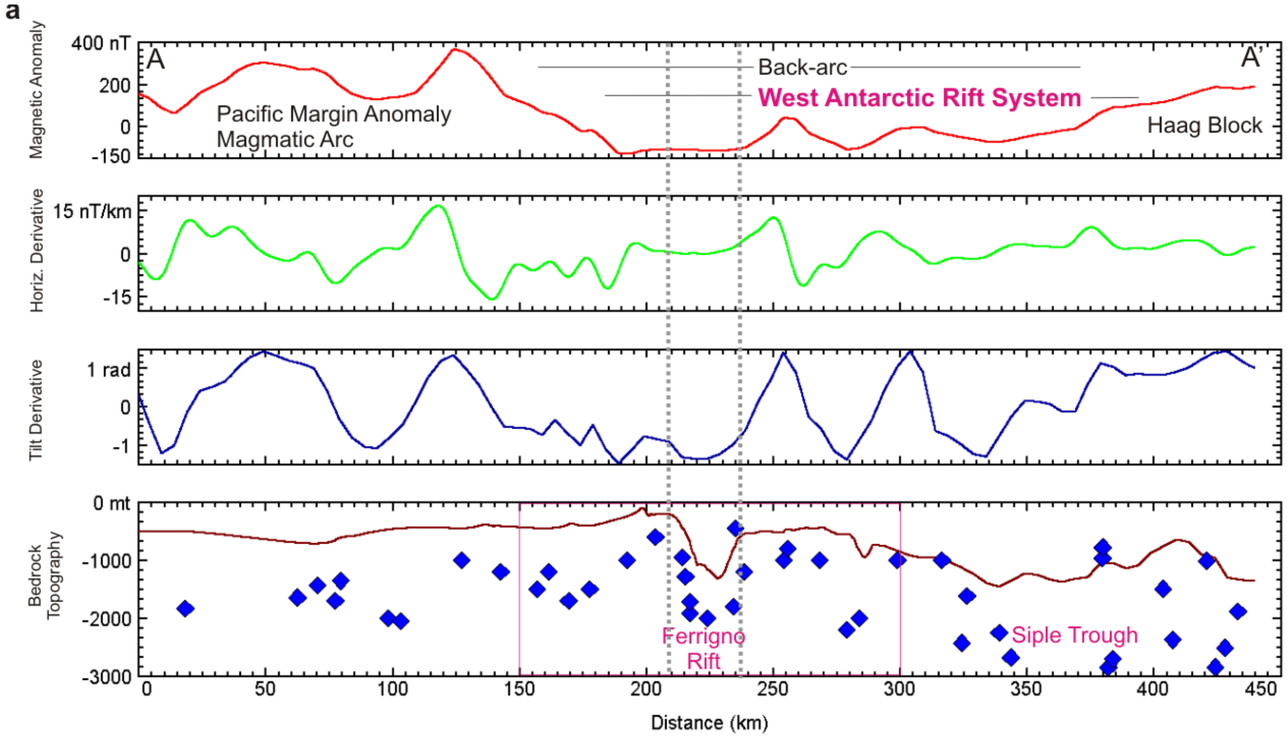

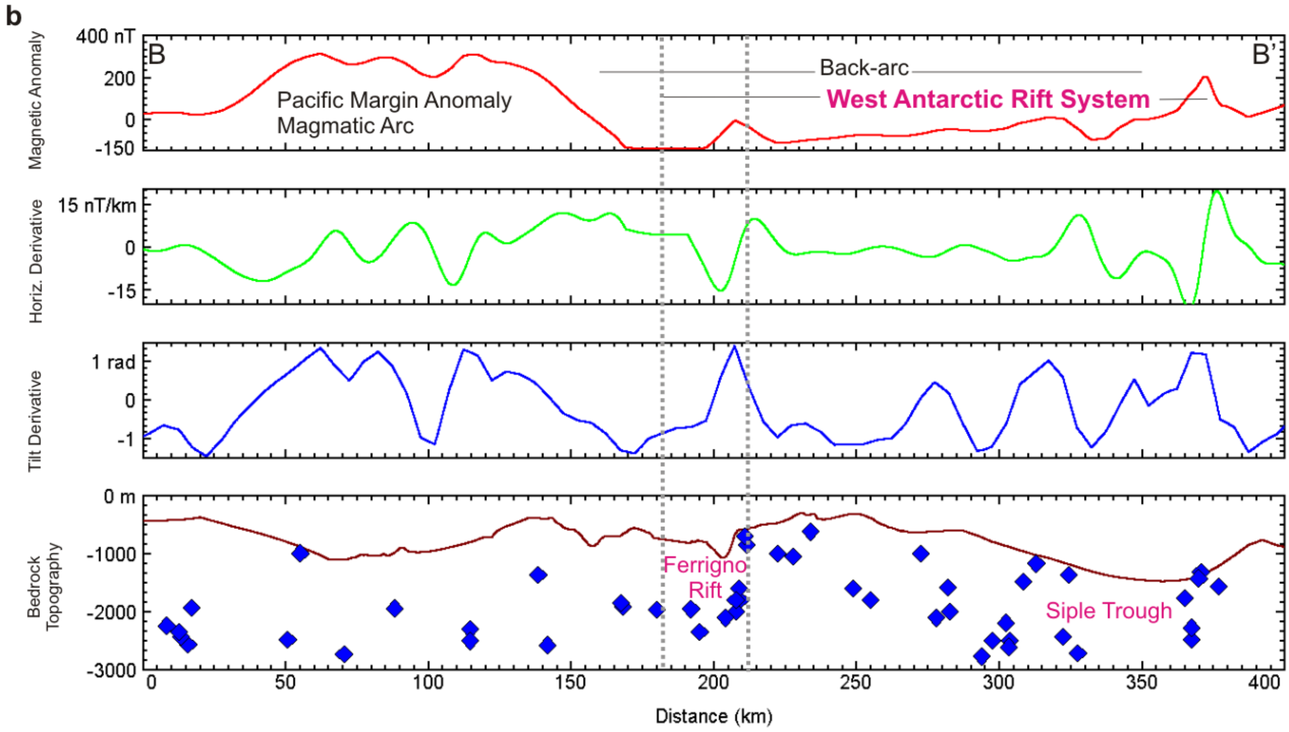

Supplementary Figure 8, parts a and b. Caption for these figures on following page.

c

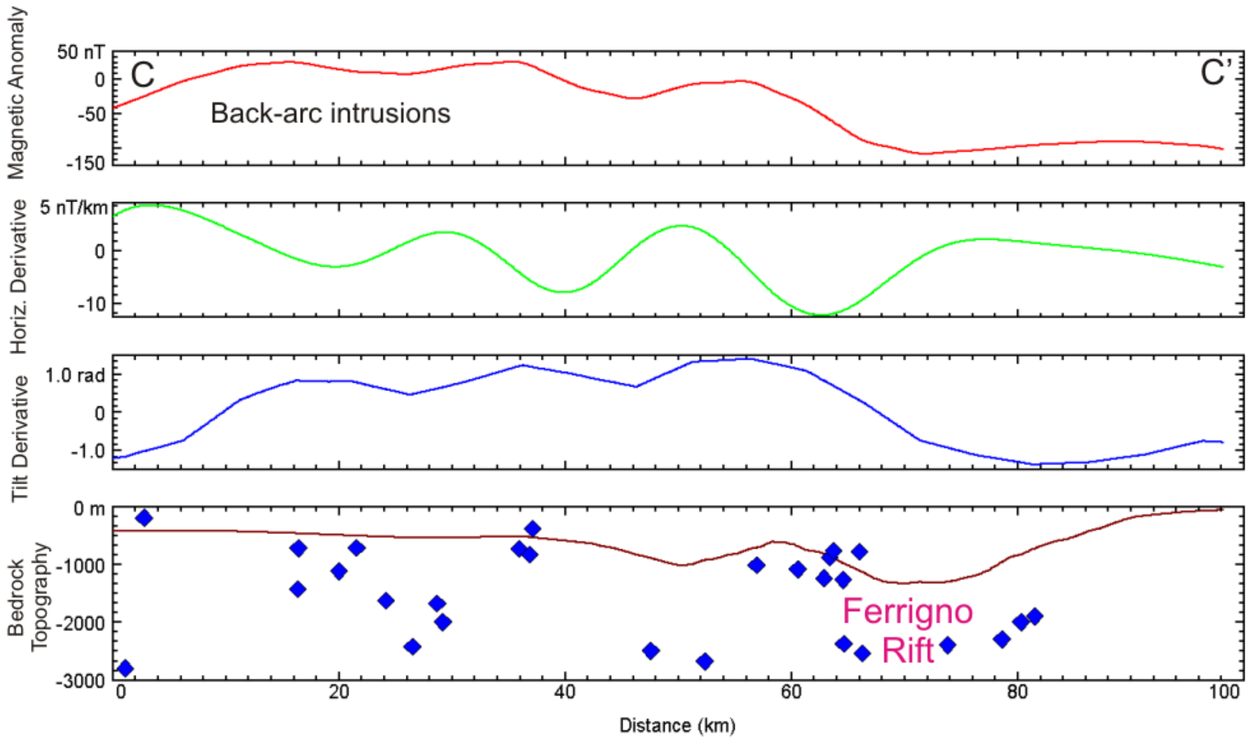

Supplementary Figure 8. Depth to magnetic source estimates for the northeastern segment of the West Antarctic Rift System, including the Ferrigno Rift. We used two-dimensional Werner Deconvolution techniques (see Ref. 48 for a description of the method) to estimate the depth to magnetic sources for profiles A-A', B-B- and C-C' that are shown in panels a, b and c respectively.

Note that over the quiet magnetic region overlying the Ferrigno Rift the method suggests clusters of solutions (diamonds) at 1 km below bedrock and this is interpreted as providing a proxy for the possible thickness of the sedimentary infill within the rift. The results of our depth to source estimates were then imported into our 2D forward gravity and magnetic models for the Ferrigno Rift region (see also Figure 3d).

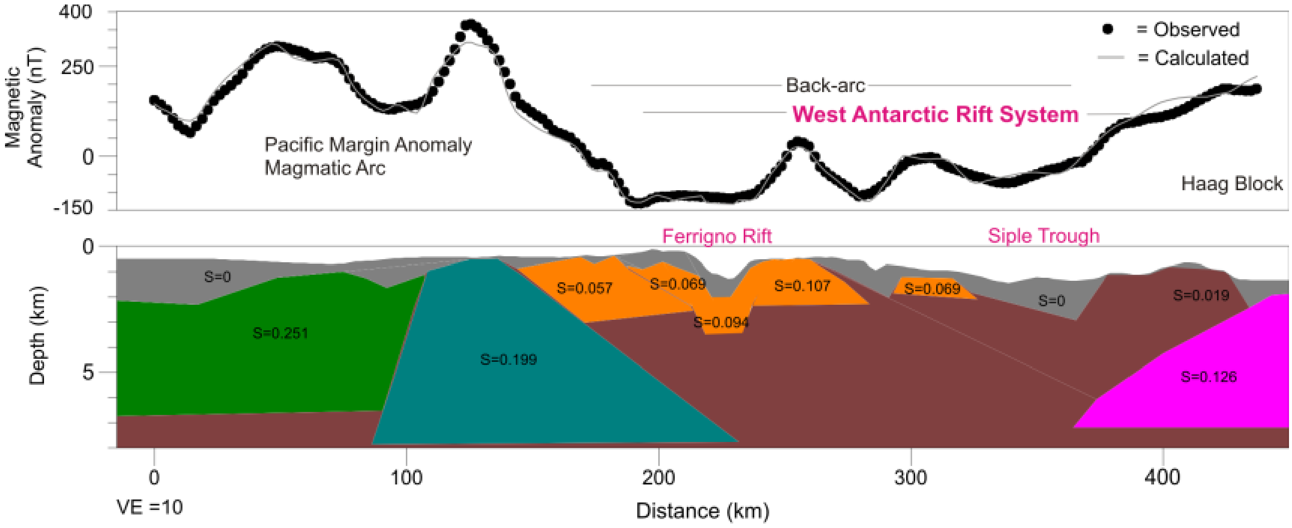

Supplementary Figure 9. Magnetic model across the northeastern segment of the West Antarctic Rift System. With the aid of two-dimensional magnetic modelling we constructed a simple upper crustal model. The labels show the apparent magnetic susceptibilities we used for the bodies expressed in SI units. The Pacific Margin Anomaly fits with 5-8 km thick magmatic arc intrusions, while relatively thinner (ca. 1-2 km thick) and more weakly magnetic intrusions are modelled in the interpreted back-arc region. At the edge of the model domain a highly magnetic block is interpreted as the leading edge of the Precambrian Haag Block. A ca. 1 km thick sedimentary layer with no apparent magnetic susceptibility is modelled within the Ferrigno Rift. Note that, according to depth to magnetic source estimates (Supplementary Figure 8) and modelling, sedimentary infill is also inferred in the broader Siple Trough region.

Supplementary Figure 10 (overleaf). Subglacial topography and estimated crustal thickness for the northeastern segment of the West Antarctic Rift System.

a, Detailed view of the subglacial topography of the West Antarctic Rift System and example profiles (solid thin white lines) located further in the interior of the rift, compared to the Ferrigno Rift (see Supplementary Figure 11).

The yellow circle shows the location of the only available independent estimate of crustal thickness from receiver function analysis for the Bentley Subglacial Trench region[71]. The dashed white lines show the inferred boundaries between the Thurston Island, Ellsworth-Whitmore and Antarctic Peninsula crustal blocks[53].

b, Detailed view of the crustal thickness as estimated from airborne gravity and satellite gravity data (see also Supplementary Figure 1c). Note that the Ferrigno Rift (which cannot be resolved from satellite gravity data alone) lies on strike with a region of thinned crust associated with the Bentley Subglacial Trench, and is also roughly parallel to a region of thinned crust identified in the northern part of the Pine Island Rift[23].

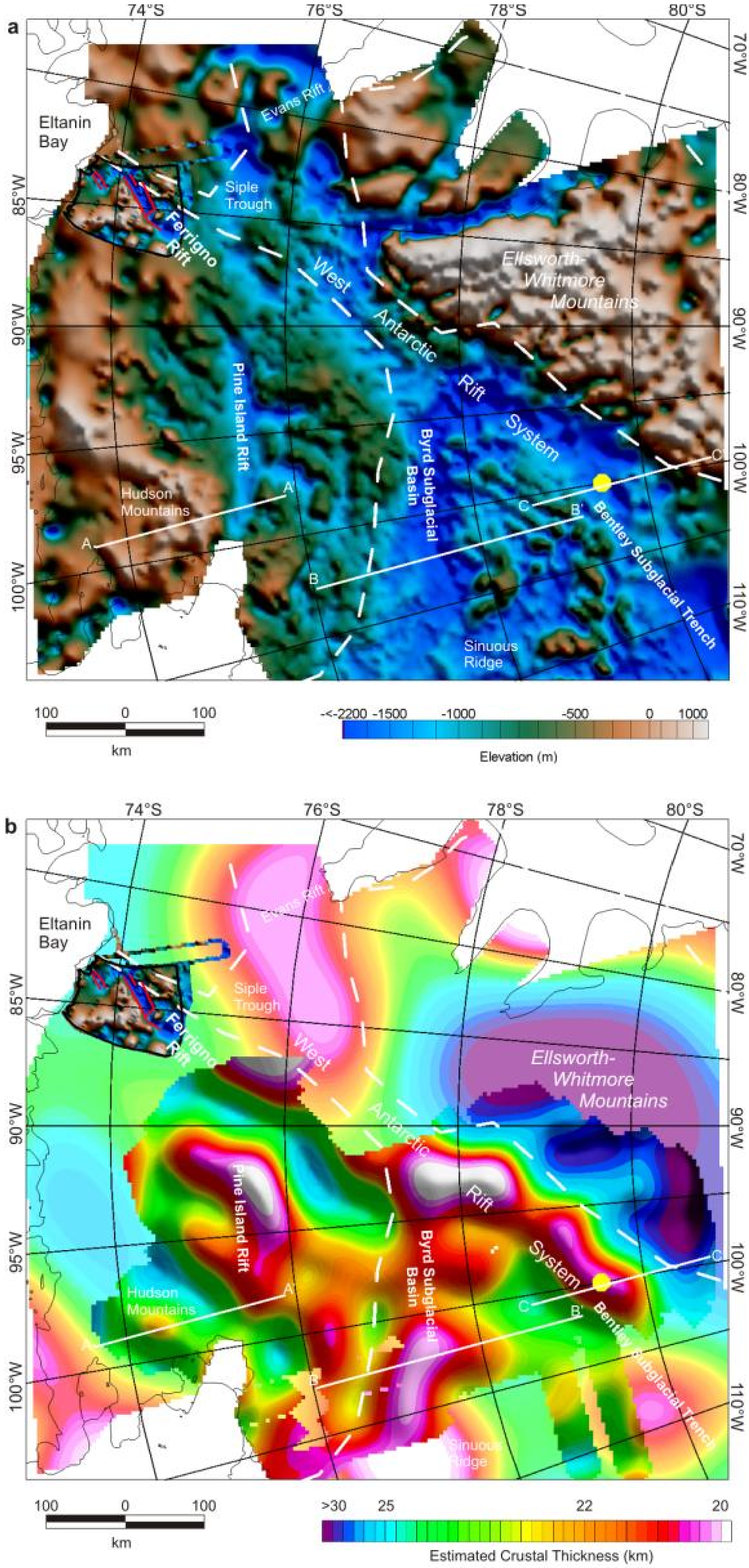

Supplementary Figure 10 (full caption on previous page).

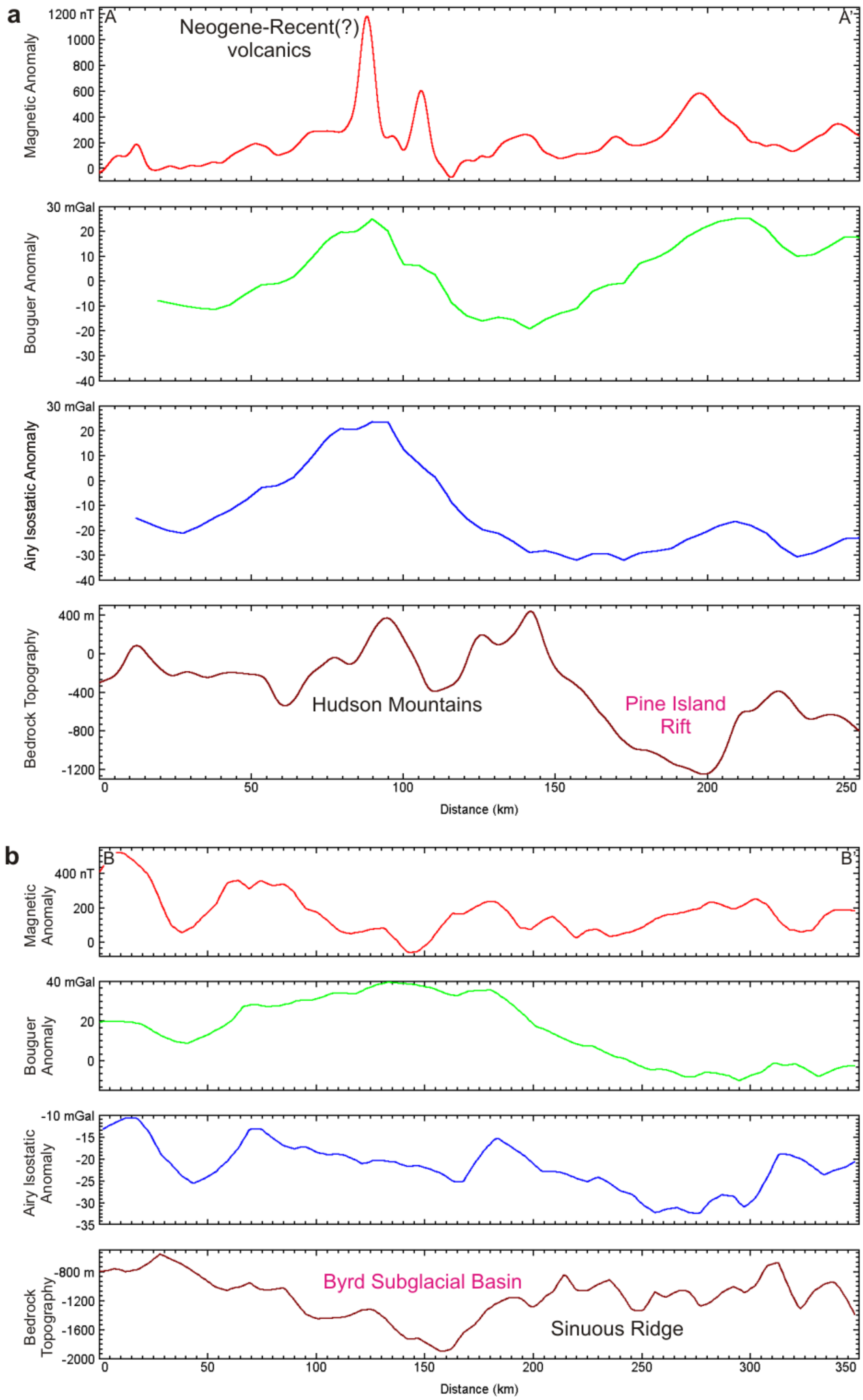

Supplementary Figure 11, parts a and b. Caption for these figures on following page.

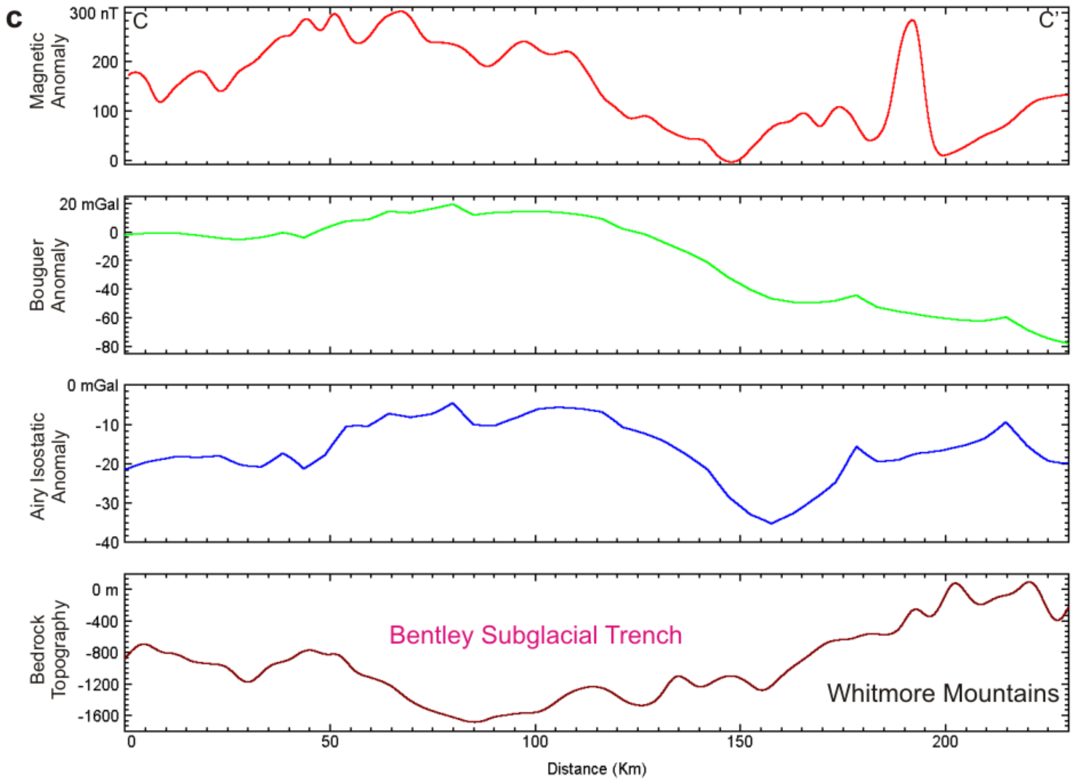

Supplementary Figure 11. Magnetic, gravity and suglacial topography data for the Pine Island Rift, Byrd Subglacial Basin and Bentley Subglacial Trench regions of the West Antarctic Rift System.

a, Profile view along section A-A' crossing the Hudson Mountains and Pine Island Rift. The upper panel shows typical high amplitude and short wavelength magnetic anomalies attributed to Neogene-Recent(?)[49,51] volcanism associated with the West Antarctic Rift System. Comparable anomalies are not detected from reconnaissance aeromagnetic data for the Ferrigno Rift region, suggesting that Cenozoic volcanism is unlikely to be as widespread as observed in the Hudson Mountains and Pine Island Rift.

Also note the airborne gravity signatures over the Pine Island Rift region. Here a high-amplitude positive Bouguer anomaly over the rift has been modelled as arising from significant crustal thinning[25]. The Airy isostatic high over the flanking Hudson Mountains is likely to reflect dense (mafic) rocks associated with Cenozoic volcanics and intrusions[23].

Note that there is no comprehensive airborne gravity survey for the Ferrigno Rift region and this precludes direct comparisons between the gravity patterns over the two regions of the WARS.

b, Profile view along section B-B' crossing the Byrd Subglacial Basin and flanking Sinuous Ridge. This section highlights the potential field signatures across the broader Byrd Subglacial Basin. A region of more distributed crustal thinning is inferred from the longer wavelength (over 100 km) Bouguer anomaly high over the basin. Note that some Airy isostatic anomalies correspond to high amplitude magnetic highs and are likely to reflect widespread subglacial Cenozoic magmatism in this part of the WARS.

c, Profile view across section C-C' crossing the Bentley Subglacial Trench. Here high-frequency magnetic anomalies suggest the occurrence of widespread Cenozoic magmatism. The Bouguer anomaly data clearly image the transition from the thinner crust typical of the WARS (more positive values) to the thicker crust beneath the Whitmore Mountains that form the rift flank. A similar long-wavelength trend is also detected from satellite gravity data moving southwards from the Ferrigno Rift and Siple Trough regions within the WARS towards the Ellsworth Mountains rift flank.

doi:10.1038/nature11292

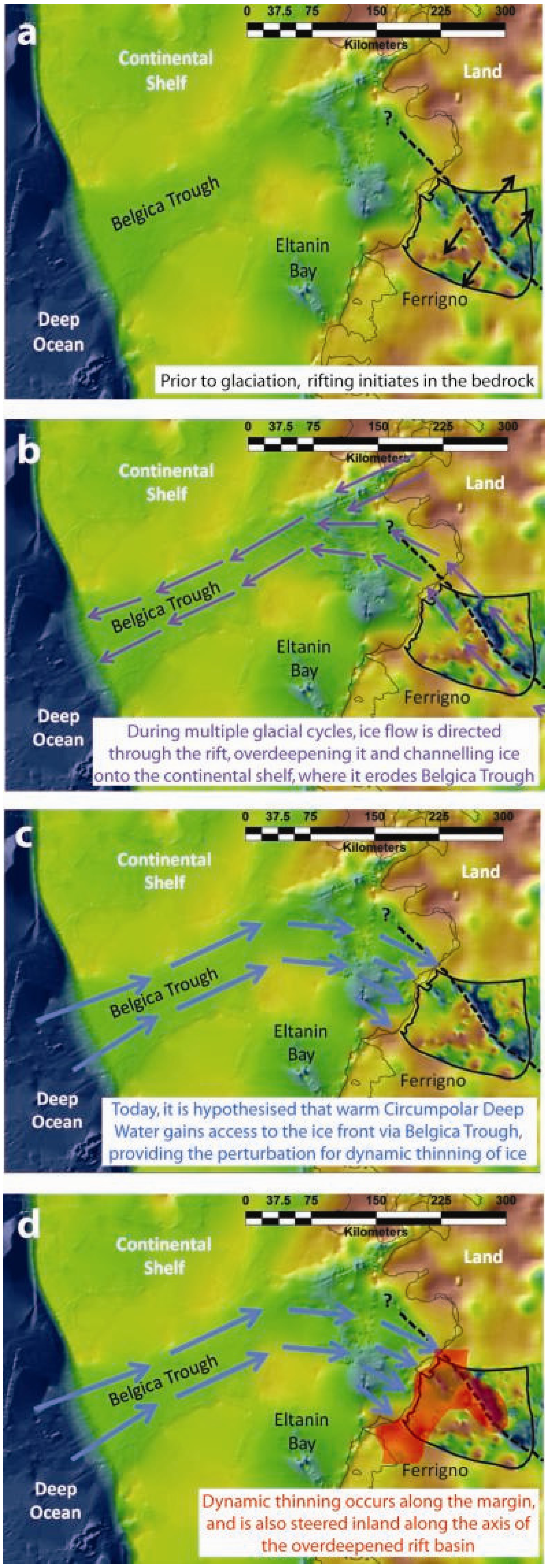

Supplementary Figure 12. Conceptual model of the opening of the Ferrigno Rift and its impact on today's ice-ocean interaction. In each panel, today's subglacial topography from refs. 29 and 30 is annotated with the Ferrigno catchment (black polygon) and arrows colour-coded in association with explanatory text.

Supplementary References

31. Holt, J.W. *et al.* New boundary conditions for the West Antarctic Ice Sheet: subglacial topography of the Thwaites and Smith Glacier catchments. *Geophys. Res. Lett.* **33**, L09502 (2006).
32. Behrendt, J.C. Crustal and lithospheric structure of the West Antarctic Rift System from geophysical investigations - a review. *Global Planet. Change*, **23**, 25-44 (1999).
33. Davey, F.J. & Brancolini, G. The late Mesozoic and Cenozoic structural setting of the Ross Sea region, in Cooper, A.K., Barker, P.F. & Brancolini, G. (eds.), Geology and seismic stratigraphy of the Antarctic Margin, *Antarctic Research Series*, **68**, Washington DC: AGU, 167-182 (1995).
34. Trey, H. *et al.* Transect across the West Antarctic rift system in the Ross Sea, Antarctica. *Tectonophysics*, **301**, 61-74 (1999).
35. Reitmayr, G. Gravity studies of Victoria Land and adjacent oceans, Antarctica, in Ricci C.A. (ed.) *The Antarctic region: geological evolution and processes*, Siena: Museo Nazionale dell' Antartide, 597-602 (1997).
36. Karner, G.D., Studinger, M. & Bell, R.E. Gravity anomalies of sedimentary basins and their mechanical implications: Application to the Ross Sea basins, West Antarctica. *Earth Planet. Sci. Lett.* **235**, 577-596 (2005).
37. Decesari, R.C., Wilson, D.S., Luyendyk, B.P. & Faulkner, M. Cretaceous and Tertiary extension throughout the Ross Sea, Antarctica, in Cooper, A. *et al.* (eds.), *Antarctica – a Keystone in a Changing World* – Online Proceedings of the 10th ISAES, Short Research Paper **098**, 6 pp.; doi: 0.3 33/of2007-1047.srp098 (2007).
38. Behrendt, J.C. *et al.* Patterns of Late Cenozoic volcanic and tectonic activity in the West Antarctic Rift System revealed by aeromagnetic surveys. *Tectonics*, **15**, 660-676 (1996).
39. Ferraccioli, F. & Bozzo, E. Cenozoic strike–slip faulting from the eastern margin of the Wilkes Subglacial Basin to the western margin of the Ross Sea Rift: an aeromagnetic connection, in Storti, F., Holdsworth, R.E. & Salvini, F. (eds.), Intraplate Strike–slip Deformation. *J. Geol. Soc. Spec. Publ.*, **210**, 109–133 (2003).
40. Ferraccioli, F. *et al.* Magmatic and tectonic patterns over the Northern Victoria Land sector of the Transantarctic Mountains from new aeromagnetic imaging. *Tectonophysics*, **478**, 43–61 (2009).
41. Decesari, R.C. *et al.* Regional seismic stratigraphic correlations of the Ross Sea: Implications for the tectonic history of the West Antarctic Rift System, in Cooper, A. *et al.* (eds.), *Antarctica – a Keystone in a Changing World* – Online Proceedings of the 10th ISAES, Short Research Paper **052**, 4 pp.; doi:10.3133/of2007-1047.srp052 (2007).
42. Siddoway, C.S., Baldwin, S., Fitzgerald, P., Fanning, C.M. & Luyendyk B.P. Ross Sea mylonites and the timing of intracontinental extension within the West Antarctic Rift System. *Geology*, **32**, 57-60 (2004).
43. Winberry, P.J. & Anandakrishnan S. Seismicity and neotectonics of West Antarctica. *Geophys. Res. Lett.* **30**, 1931 (2003).
44. Wannamaker, P.E., Stodt, J.A. & Olsen, S.L. Dormant state of rifting below the Byrd Subglacial Basin, West Antarctica, implied by magnetotelluric (MT) profiling. *Geophys. Res. Lett.* **23**, 2983-2986 (1996).
45. Donnellan, A. & Luyendyk, B. GPS evidence for a coherent Antarctic plate and for postglacial rebound in Marie Byrd Land. *Global Planet. Change*, **42**, 305– 311 (2004).
46. Busetti, M., Spadini, G., van der Wateren, F.M., Cloetingh, S. & Zanolla, C. Kinematic modelling of the West Antarctic Rift System, Ross Sea, Antarctica. *Global Planet. Change*, **23**, 79–103 (1999).
47. Bell, R.E., Studinger, M., Karner, G., Finn, C.A., & Blankenship, D.D. Identifying major sedimentary basins beneath the West Antarctic Ice Sheet from aeromagnetic data analysis, in Fütterer, D.K. *et al.* (eds.), *Antarctica: Contributions to Global Earth Sciences*. Berlin: Springer, 117-121 (2006).
48. Ku, C.C. & Sharp, J.A. Werner deconvolution for automated magnetic interpretation and its refinement using Marquardt inverse modelling. *Geophysics*, **48**, 754–774 (1983).
49. LeMasurier, W.E. & Thomson, J. W. Volcanoes of the Antarctic Plate and Southern Oceans, *Antarctic Research Series*, Vol. 48, Washington DC: AGU, 512 pp. (1990).
50. Blankenship, D.D. *et al.* Active volcanism beneath the West Antarctic Ice Sheet and implications for ice-sheet stability. *Nature*, **361**, 526-529 (1993).
51. Corr, H.F.J. & Vaughan, D.G. A recent volcanic eruption beneath the West Antarctic ice sheet: *Nature Geosc.*, **1**, 122-125 (2008).

52. Behrendt, J.C., Finn, C.A., Blankenship, D. & Bell, R.E. Aeromagnetic evidence for a volcanic caldera(?) complex beneath the divide of the West Antarctic Ice Sheet. *Geophys. Res. Lett.* **25**, 4385-4388 (1998).
53. Dalziel, I.W.D. & Elliot D.H. West Antarctica: problem child of Gondwanaland. *Tectonics*, **1**, 3-19 (1982).
54. Eagles, G., Gohl, K. & Larter, R.D. Animated tectonic reconstruction of the Southern Pacific and alkaline volcanism at its convergent margins since Eocene times. *Tectonophysics*, **464**, 21-29 (2009).
55. Ferraccioli, F., Jones, P.C., Vaughan, A.P.M. & Leat, P.T. New aerogeophysical view of the Antarctic Peninsula: More pieces, less puzzle. *Geophys. Res. Lett.* **33**, L05310 (2006).
56. Eagles, G., Larter, R.D., Gohl, K. & Vaughan, A.P.M. West Antarctic Rift System in the Antarctic Peninsula. *Geophys. Res. Lett.* **36**, L21305 (2009).
57. Davey, F.J., Cande, S.C. & Stock, J.M. Extension in the western Ross Sea region - links between Adare Basin and Victoria Land Basin. *Geophys. Res. Lett.* **33**, L20315 (2006).
58. Cande, S.C., Stock, J.M., Müller, R.M. & Ishihara, T. Cenozoic motion between East and West Antarctica. *Nature*, **404**, 145-150 (2000).
59. Henrys, S., *et al.* Tectonic history of mid-Miocene to present southern Victoria Land Basin, inferred from seismic stratigraphy in McMurdo Sound, Antarctica, in Cooper, A. *et al.* (eds.), *Antarctica – a Keystone in a Changing World* – Online Proceedings of the 10th ISAES, Short Research Paper **049**, 4 pp.; doi:10.3133/of2007-1047.srp049 (2007).
60. Bosum, W., Damaske, D., Roland, N.W., Behrendt, J.C. & Saltus, R. The GANOVEX IV Victoria Land/Ross Sea aeromagnetic survey: interpretation of the anomalies. *Geologisches Jahrbuch* **E38**, 153–230 (1989).
61. Ferraccioli, F., Bozzo, E. & Damaske, D. Aeromagnetic signatures over western Marie Byrd Land provide insight into magmatic arc basement, mafic magmatism and structure of the eastern Ross Sea Rift flank, *Tectonophysics*, **347**, 139-165 (2002).
62. Sweeney, R.E., Finn, C.A., Blankenship, D.D., Bell, R.E. & Behrendt, J.C. Central West Antarctica aeromagnetic data: a web site for distribution of data and maps (on-line edition). *U.S. Geological Survey Open-File Report* 99-0420 (1999).
63. Golynski, A.V. *et al.* ADMAP - Magnetic anomaly map of the Antarctic, 1:10,000 scale map. *BAS Miscellaneous Series*, Map 10, Cambridge: British Antarctic Survey (2001). http://www.antarctica.ac.uk/about_antarctica/geography/maps/admap.php
64. Behrendt, J.C. *et al.* Casertz aeromagnetic data reveal late Cenozoic flood basalts(?) in the West Antarctic Rift System. *Geology*, **22**, 527-530 (1994).
65. Behrendt, J.C., Blankenship, D.D., Morse, D.L. & Bell, R.E. Shallow-source aeromagnetic anomalies observed over the West Antarctic Ice Sheet compared with coincident bed topography from radar ice sounding - new evidence for glacial ‘‘removal’’ of subglacially erupted late Cenozoic rift-related volcanic edifices. *Global Planet. Change*, **42**, 177–193 (2004).
66. Vogel, S.W. *et al.* Geologic constraints on the existence and distribution of West Antarctic subglacial volcanism. *Geophys. Res. Lett.* **33**, L23501 (2006).
67. Rocchi, S. *et al.* Cenozoic magmatism in the western Ross Embayment: role of mantle plume versus plate dynamics in the development of the West Antarctic Rift System. *J. Geophys. Res.* **107**, 2195 (2002).
68. Vogel, S.W. & Tulaczyk S. Ice-dynamical constraints on the existence and impact of subglacial volcanism on West Antarctic ice sheet stability. *Geophys. Res. Lett.* **33**, L23502 (2006).
69. Hathway, B. Sims Island: first data from a Pliocene alkaline volcanic centre in eastern Ellsworth Land. *Antarctic Sci.* **13**, 87-88 (2001).
70. Finn, C.A., Müller, R.D. & Panter, K.S. A Cenozoic diffuse alkaline magmatic province (DAMP) in the southwest Pacific without rift or plume origin. *Geochem. Geophys. Geosys.* **6**, Q02005 (2005).
71. Winberry, J.P. & Anandakrishnan S. Crustal structure of the West Antarctic Rift System and Marie Byrd Land hotspot. *Geology*, **32**, 977-980 (2004).
72. Ferraccioli, F., *et al.* East Antarctic rifting triggers uplift of the Gamburtsev Mountains. *Nature*, **479**, 388-392 (2011).
73. Gohl, K. *et al.* Geophysical survey reveals tectonic structures in the Amundsen Sea embayment, West Antarctica. *in Cooper, A. et al. (eds.), Antarctica – a Keystone in a Changing World* – Online Proceedings of the 10th ISAES, Short Research Paper **047**, 4 pp., doi:10.3133/of2007-1047 (2007).

74. Jones, P.C., Johnson, A.C., von Frese, R.R.B. & Corr, H. Detecting rift basins in the Evans Ice Stream region of West Antarctica using airborne gravity data. *Tectonophysics*, **347**, 25-41 (2002).
75. Ferraccioli F., Gambetta, M. & Bozzo, E. Microlevelling precedures applied to regional aeromagnetic data: an example from the Transantarctic Mountains (Antarctica), *Geophys. Prospect.*, **46**, 177-196 (1998).
76. Cooper, G.R.J. & Cowan, D.R.. Enhancing potential field data using filters based on the local phase. *Comput. Geosc.* **32**, 1585–1591 (2006).